Doctoral Dissertation

(Shinshu University)

Preparation of bio-based polymeric nanocomposite scaffolds for advanced biomedical applications

バイオメディカル応用を目的としたバイオベースの高分子ナノコンポジット足場の作製

March 2022

EL-GHAZALI SOFIA
19hb201h

Supervisor: Professor Shunichi Kobayashi

Department: Biomedical Engineering

ABSTRACT

Preparation of bio-based polymeric nanocomposite scaffolds for advanced biomedical applications

Nanofibers are very porous materials with a high surface area. Therefore, they are the most suitable textile materials for scaffolding application as their morphological structure is similar to that of the human extra cellular matrix.

Medical textiles are emerging and quickly developing in the biomedical sector starting from basic wound dressing materials to scaffolds intended for use in typical surgical operations. Current studies reveal that the bio-based polymeric electrospun nanofiber mats (ENMs) have gained great attention for the fabrication of biomaterials. However, the improvement in mechanical properties of such materials has remained a big research gap.

Conventionally, polyesters are not considered eco-friendly materials due to their petroleum origin and their slow degradation in the landfill. However, they are abundantly present in our daily life and researchers found that they can benefit human health when applied as biomaterials for regenerative medicine. Polycyclohexylenedimethylene (PCT) is a type of polyesters with very good mechanical properties, but it has been challenged by the constraint of the very high temperature required for its processing.

Isosorbide has attracted a great deal of attention due to its biocompatibility, biodegradability, non-toxicity, and its wide abundance on earth. The introduction of this monomer by a synthesis method has contributed in overcoming the aforementioned problem and lowering the processability temperature of PCT.

This thesis covers two main studies related to biomedical applications starting with our first project that states the possibility to apply polyester materials incorporated with Isosorbide derived from corn glucose in the biomedical field. We prepared Poly (Ethylene-glycol-co-1,4-Cyclohexane di-methylene-co-isosorbide terephthalate) (PEICT) and Poly (1, 4 cyclohexane di-methylene-co-isosorbide terephthalate) (PICT) nanofibers as well as their blended composition (BLEND) for the first time and we could successfully manufacture these three types of nanofibers in the form of artificial blood vessels (ABV) with different diameters using electrospinning technique, we also underwent a detailed characterization of the resultant scaffolds. Interestingly, a compacted morphology and enhanced wettability were imparted onto the surface of BLEND ABVs. In addition, BLEND has showed a comparatively higher

biodegradation rate in parallel to tunable tensile strength. Thus, the fabricated BLEND composite scaffolds tend to be promising for application in the biomedical field.

In our second project, we focused on the preparation of PEICT ENMs to further investigate the reason of the low cell infiltration, thus we produced PEICT ENMs at a higher polymer concentration to obtain nanofibers with a bigger average diameter for the infiltration of fibroblast cells. PEICT ENMs showed very good cell adhesion and viability revealing its potential to be used as biomaterials.

From the first main study of this thesis, it was observed that the surface properties of polymeric materials can be modified by a simple blend electrospinning. Therefore, we tried to explore the surface properties of two bio-based polymers, namely Polyglycolic acid (PGA) and Collagen for an intended application in surgical procedures with an improvement in handling properties. It was concluded that PGA/collagen (60:40) was the optimal blend ratio which resulted in nanofibers with improved surface wettability, which is ultimately good for cell adhesion.

Keywords: Nanofibers, biomedical, cell culture, scaffold, Poly(Ethylene-glycol 1,4-Cyclohexane Dimethylene-Isosorbide-Terephthalate), poly (1, 4 cyclohexane di-methylene-co-isosorbide terephthalate), Polyglycolic Acid, Collagen, blending

TABLE OF CONTENTS

CHAPTER 1 General Introduction

1.1 Background and Literature

Bio-based polymers have gained a great deal of attention due to their unique properties of breathability and biodegradability and widespread applications in smart sensors, advanced textiles, energy, environment and biomedical applications. Therefore, in this research we focused on the fabrication of blended composites from different polymers and explored their biomedical potential in the light of chemical, morphological and surface properties.

Electrospinning is a well-known technique for easy fabrication of both pristine and blended polymeric nanofibers. As polymers, we utilized two types of Isosorbide-based polyesters, Polyglycolic acid and Collagen and we explored their biocompatibility and other related characteristics for three research projects of this thesis. Polymeric compositions in the form of nanofibers are very popular for their utilization in biomedical applications including wound dressing, cell culture and surgical operations. Nanofibers have been also applied to various other fields to date, including aerospace, environment, sensors, agriculture, filtration, face masks against bacteria, pollen and viruses, batteries, cosmetics, food, pharmaceutical, surgical gowns and advanced apparels.

Polymer blends are materials containing at least two combined polymers with different physical properties. They are versatile and offer synergism in properties for a broad range of applications [1]. Owing to the advancement of nanotechnology, new features can be added to medical textiles by blending nanoscale materials into conventional textile products [2].

Electrospun nanofiber blends are widely used as biomaterials for different applications, such as tissue engineering and cell adhesion. With a focus on eco-friendly materials, the second and third chapters of this thesis contain experimental studies on PICT and PEICT, both originated from PCT which is one of the most widely used aromatic polyesters with high mechanical properties, copolymerized with Isosorbide as a bio-based monomer [3].

A growing interest has been observed for Collagen and Polyglycolic acid (PGA) based nano compositions. PGA is one of the green polymers [4,5] with very good mechanical strength, temperature resistance, biodegradability and biocompatibility [5-8]. PGA nanofibers have unique scaffolding characteristics which make them highly suitable to be used for biomedical and tissue engineering applications [9,10,11]. Collagen has similar properties, but its nanofibers do not have enough strength. In addition to biodegradability, biocompatibility and low immunogenicity, Collagen has very good hydrophilicity which can be ultimately

advantageous for cell adhesion [12]. The fourth chapter of this thesis describes a study of nanofibers based on PGA and Collagen under different surface treatment conditions.

1.2 Electrospun Nanofibers

Electrospinning is a well-known nanofiber production technique which consists of supplying a high voltage to a polymeric solution and collect nanofibers on an oppositely charged collector. The resulting nanofibers are then dried and peeled off for further characterizations.

Currently, electrospinning is considered an efficient method for manufacturing continuous nanofibers which can be prepared from pristine/blend natural and synthetic polymers. The possibility of incorporation of any external material such as nanoparticles, drugs, nanosheets or any natural ingredients on nanofibers is an additional advantage of using electrospinning technique [14, 15].

Many types of collectors can be used for electrospinning depending on the requirements of nanofibers morphology and the collectors can be kept either stable or in motion. For instance, a high-speed rotating cylinder can form aligned nanofibers depending on the average diameter size of nanofibers and the rotating speed, while parallel stable metallic rods can be used to collect highly aligned nanofibers [16]. In our research we have used metallic rods to manufacture tubular nanofibers in the form artificial blood vessels as shown in Fig. 1.1. We have also utilized a cage-type metallic collector to obtain an improved texture on the surface of PGA/Collagen resultant nanofibrous mats as shown in Fig. 4.1.

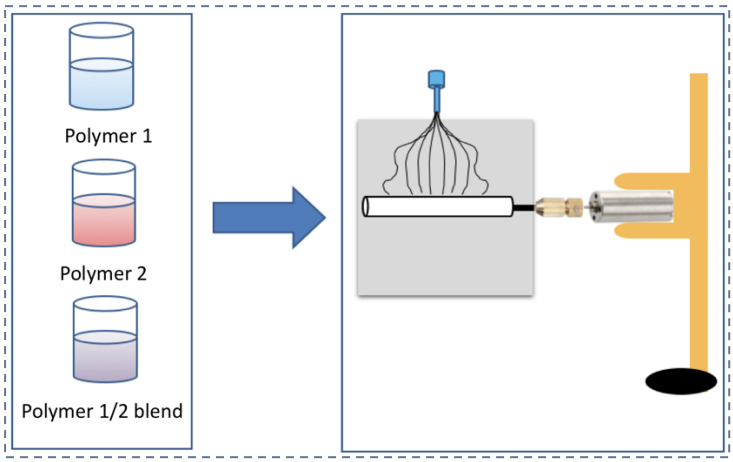

Fig. 1.1. Electrospinning process for the preparation of tubular Polymer 1 and polymer 2 nanofibers using a mechanical setup for rotary motion transfer.

1.3 Nanofibers in biomedical application

In biology, the sizes of most features existing in Natural Extra Cellular Matrix (NECM) such as ridges and pores are in the nanometer range [16,17] and cells attach well around fibers with diameters smaller than the diameter of the cells, i.e. the nanometer range [18]. Consequently, the NECM provides excellent structural and biochemical support for the surrounding cells. Similarly, in vitro, cells interact with signals from their culture environment, that physical and chemical properties of which strongly influence cell activities. Therefore, it is very necessary to mimic the nanoscale structures existing in NECM while creating a polymeric synthetic Extra Cellular Matrix (ECM) scaffold for tissue replacement and provide a highly porous three dimensional substrate that mimics the native ECM that can accurately interact with cells. Nanofibers produced by electrospinning represent a promising candidate 3D scaffold that have been developed to fulfill the requirements for tissue engineering applications as they morphologically resemble the fibrillar components of the native ECM since they can enhance cell adhesion, proliferation, and differentiation. These fibers possess unique physical characteristics, such as high surface area to volume ratio and improved mechanical strength which make them well suited as tissue engineering scaffolds for various tissue types, mainly musculoskeletal tissues such as cartilage, bone, tendon, ligament, skin tissues, vascular tissues, neural tissues, and as carriers for the controlled delivery of drugs, proteins, and DNA.

1.4 Polyester nanofibers containing the bio-based monomer Isosorbide

PICT and PEICT are eco-friendly nanofibers in form of polyester nanofibers containing Isosorbide. This latter is a stereoisomer of 1,4:3,6-dianhydrohexitol. It is considered as the most favored candidate for renewable monomers used in addressing environmental issues, thanks to its polymer synthesis accessibility. [19]

1.5 PGA and Collagen polymers

PGA is a biocompatible material [20-22] with excellent properties, it has a high thermal stability, high mechanical strength, and it is rapidly biodegradable [23]. Nonwoven nanofibrous PGA mats/webs have been extensively used in scaffolding for tissue regeneration due to their excellent degradability, and cell viability [24].

Collagen is a structural protein of the extracellular matrix (ECM) which is the most abundant protein in mammals [25]. Collagen-based biomaterials are valuable because of their biocompatibility [26], and biodegradability, as well as their ability to support tissue/cell adhesion and cell proliferation [27]. Collagen is one of the most useful biopolymers because of its low immunogenicity [28]. Due to their biomimetic and structural composition in the extracellular matrix (ECM), collagen-based biomaterials are widely applied in tissue regeneration [29].

1.6 Importance of the vascular graft research

Atherosclerotic cardiovascular disease (ACD) illustrated in Fig. 1.2. is a leading cause of death worldwide. The current therapy of this disease consists of vascular replacement which can be operated using different methods. The most standard material used to potentially replace a clogged blood vessel remains the patient's own blood vessel, commonly known as bypass graft. However, the availability and safety of this material is not guaranteed in all cases. The second option regarding this type of interventions is the commercially available vascular prostheses, such as Dacron (polyethylene terephthalate (PET)) and Teflon (expanded polytetra-fluoroethylene (ePTFE)), which remarkably fulfill the desired function for large-caliber replacements, but their drawback lies in small-caliber applications (i.e. I.D. $\leq$6 mm), due to the long-term patency caused by hemodynamic disturbances leading to surface thrombogenicity. In fact, Small-diameter grafts of both Dacron and Teflon failed rapidly due to occlusion and when used to bypass arteries showed rates of thrombosis greater than 40% after 6 months [30]. Some attempts have been done to increase graft patency, such as coatings using protein to minimize the interactions between blood and the foreign biomaterial. Luminal seeding of synthetic grafts with different cells is also an attempt to create a living hemo-compatible environment. Despite of the promising initial results of these processes, an ideal solution is not available yet as artificial materials are still a potential risk for microbial infections. As an idea to overcome the mentioned limitations, cardiovascular tissue engineering is a new approach to manufacture fully autologous temporary substitutes of blood vessels that interact with cells of the local environment as living structures and have the potential of self-renewing and healing. In general, the natural or synthetic materials used for tissue engineering provide a temporary biomechanical structure that remain in action until the cells become independent and apt to produce their own extracellular matrix.

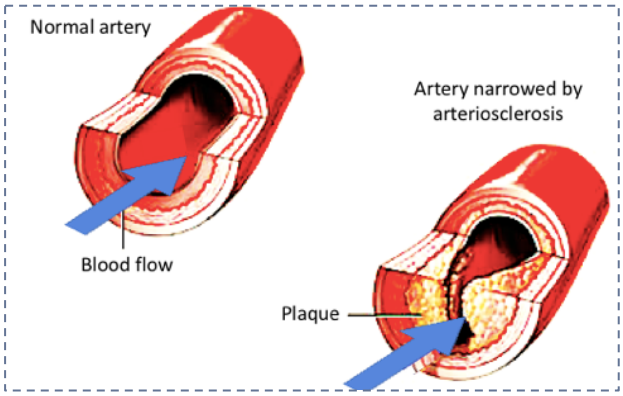

Fig. 1.2. Diagram illustrating an arteriosclerotic plaque build-up inside the blood vessel

1.7. Types of cells

Cell is by definition the smallest structural and functional unit of an organism, which is typically microscopic and consists of cytoplasm and a nucleus enclosed in a membrane. Stem cell is an undifferentiated cell of a multicellular organism, from which all organism cells which perform specialized functions viz. fibroblasts, osteoblasts, nervous cells, epithelial cells and immune cells are generated by differentiation. Fig.1.3. and Table 1.1. enlist the common primary cell types.

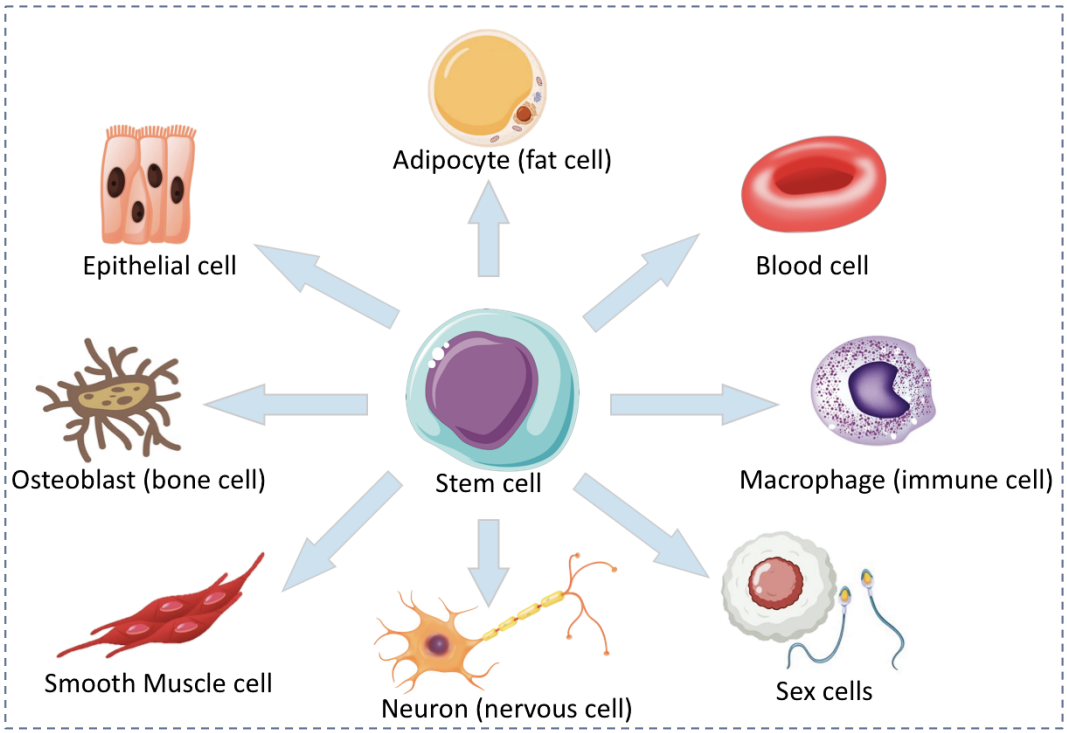

Fig. 1.3. Diagram illustrating stem cell and the main differentiated cells

Table 1.1. Common Primary Cell Types (Sigma Aldrich)

Epithelial	Endothelial	Fibroblasts	Keratinocytes	Melanocytes	Neurons
Astrocytes	Hepatocytes	Skeletal Muscle	Smooth Muscle	Osteoblasts	Myocytes
Chondrocytes	Adipocytes	Synoviocytes	Hair Cells	Blood Cells	Stem Cells

1.8 Objectives

In our research, we focused on biomedical applications of eco-friendly materials using electrospinning technique.

The main objectives of the research are listed below:

1- Fabrication of bio-based polymeric blended nanofiber compositions via electrospinning;
2- Production of small diameter artificial blood vessels from PICT, PEICT and blended nanofibers;
3- Conducting related chemical and physical characterizations;
4- Exploring the application of nanofiber mats in cell culture;
5- Assessing the extent of biodegradability of PEICT, PICT and blended nanofiber mats;
6- Optimizing and exploring PGA/Collagen blends for potential biomedical applications.

The highlighted outcomes of the research chapter-wise are given below.

CHAPTER 1

In chapter 1, an introduction to the electrospinning technique has been discussed along with the current issues related to biomaterials used in the biomedical field, and how the polymer-based materials have the potential to address these problems at some extent. An overview of the materials used in this research is also detailed.

CHAPTER 2

This work suggested new biomass polymeric nanofibers which can be used for industrial applications such as tissue engineering and scaffolding. Isosorbide is an eco-friendly natural biomaterial abundantly available on earth and best fitted for the functional textile substrates.

Bio-based polyester copolymers PICT and PEICT nanofibers were prepared in tubular shapes to mimic small diameter (<2mm) blood vessels, they were characterized and investigated for

biodegradation. we reported successful human breast cell culture and adhesion on the surface of blended composition of PICT and PECIT with the ratio 50:50.

CHAPTER 3

In this chapter, PEICT is further explored for the cell culture of fibroblast cells in parallel to cell viability. The average nanofiber diameter was increased as a results of increased polymer concentration for electrospinning of PEICT ENMs. This research clarified that the surface properties and average diameter of nanofibers play an important role for cell culture applications depending on the cell type and size.

CHAPTER 4

In chapter 1 and 2, the reason of good cell infiltration was revealed as a relationship with the surface of nanofibers, thus, in chapter 4 we tried to check the effect of surface treatments on the wettability and morphology of nanofibers surface, as these properties are considered key for cell culture applications. In this study, in lieu of conducting a simple in-vitro cell culture assay, we attempted to optimize the surface affecting parameter on biocompatible polymers, therefore, we chose two bio-based polymers, namely PGA and Collagen were blended at different ratios and 60:40 PGA/Collagen was observed as optimal blend in the context of handling properties which were further improved by using a cage-type collector for electrospinning to impart respective texture on the surface. Basically, optimized blend surface was treated using two techniques, Plasma treatment (Nitrogen) and Ozonation to improve the wettability and the treatment parameters were optimized with respect to morphological stability. The proposed method of cage-type manufacturing opens a new door to continuous electrospinning with tunable morphology, having the potential to be used for biomedical applications in the future.

1.9 References

1. Das, S., Samal, S. K., Mohanty, S., & Nayak, S. K. (2018). Crystallization of Polymer Blend Nanocomposites. In Crystallization in Multiphase Polymer Systems (pp. 313-339). Elsevier.
2. Qin, Y. (2016). Applications of advanced technologies in the development of functional medical textile materials. Medical Textile Materials, 1, 55-70.
3. D.N. Phan, H. Lee, D. Choi, C.-Y. Kang, S.S. Im, I.S. Kim, Fabrication of two polyester nanofiber types containing the biobased monomer isosorbide: poly (ethylene glycol 1,4-cyclohexanedimethylene isosorbide terephthalate) and poly (1,4-cyclohexanedimethylene isosorbide terephthalate), Nanomaterials 8 (2018) (2018) 56.
4. Lim, H.; Kim, H.S.; Qazi, R.; Kwon, Y.; Jeong, J.; Yeo, W. Advanced soft materials, sensor integrations, and applications of wearable flexible hybrid electronics in healthcare, energy, and environment. Adv. Mater. 2020, 32, 1901924.
5. Daniel, S. Biodegradable Polymeric Materials for Medicinal Applications. In Green Composites; Springer: Berlin/Heidelberg, Germany, 2021; pp. 351–372.
6. Shuai, C.; Yang, W.; Feng, P.; Peng, S.; Pan, H. Accelerated degradation of HAP/PLLA bone scaffold by PGA blending facilitates bioactivity and osteoconductivity. Bioact. Mater. 2021, 6, 490–502.
7. Sharma, U.; Concagh, D.; Core, L.; Kuang, Y.; You, C.; Pham, Q.; Zugates, G.; Busold, R.; Webber, S.; Merlo, J. The development of bioresorbable composite polymeric implants with high mechanical strength. Nat. Mater. 2018, 17, 96–103.
8. Park, K.I.; Teng, Y.D.; Snyder, E.Y. The injured brain interacts reciprocally with neural stem cells supported by scaffolds to reconstitute lost tissue. Nat. Biotechnol. 2002, 20, 1111–1117.
9. Sun, A.; He, X.; Li, L.; Li, T.; Liu, Q.; Zhou, X.; Ji, X.; Li, W.; Qian, Z. An injectable photopolymerized hydrogel with antimicrobial and biocompatible properties for infected skin regeneration. NPG Asia Mater. 2020, 12, 25.
10. Low, Y.J.; Andriyana, A.; Ang, B.C.; Zainal Abidin, N.I. Bioresorbable and degradable behaviors of PGA: Current state and future prospects. Polym. Eng. Sci. 2020, 60, 2657–2675.
11. El-Ghazali, S.; Khatri, M.; Hussain, N.; Khatri, Z.; Yamamoto, T.; Kim, S.H.; Kobayashi, S.; Kim, I.S. Characterization and biocom- patibility evaluation of artificial blood vessels prepared from pristine poly (Ethylene-glycol-co-1, 4-cyclohexane dimethylene-co-isosorbide terephthalate), poly (1, 4 cyclohexane di-methylene-co-isosorbide terephthalate) nanofi. Mater. Today Commun. 2021, 26, 102113.
12. Muzamil Khatri, Farooq Ahmed, Abdul Wahab Jatoi, Rasool Bux Mahar, Zeeshan Khatri and Ick Soo Kim "Ultrasonic Dyeing of cellulose nanofiber" Ultrasonics sonochemistry (2016), 31, 350-354
13. Phan, D.N., Rebia, R.A., Saito, Y., Kharaghani, D., Khatri, M., Tanaka, T., Lee, H. and Kim, I.S., 2020. Zinc oxide nanoparticles attached to polyacrylonitrile nanofibers with hinokitiol as gluing agent for synergistic antibacterial activities and effective dye removal. Journal of Industrial and Engineering Chemistry.
14. Qureshi, U. A., Khatri, Z., Ahmed, F., Khatri, M., & Kim, I. S. (2017). Electrospun zein nanofiber as a green and recyclable adsorbent for the removal of reactive black 5 from the aqueous phase. ACS Sustainable Chemistry & Engineering, 5(5), 4340-4351.
15. Khatri, M., Qureshi, U. A., Ahmed, F., Khatri, Z., & Kim, I. S. (2018). Dyeing of electrospun nanofibers. In Handbook of nanofibers (pp. 1-16). Springer.
16. Xu, C. Y., Inai, R., Kotaki, M., & Ramakrishna, S. (2004). Aligned biodegradable nanofibrous structure: a potential scaffold for blood vessel engineering. Biomaterials, 25(5), 877-886.

17. Abrams GA, Goodman SL, Nealey PF, Murphy CJ. Nanoscale topography of matrigel. IOVS 1998;39:5160.
18. Laurencin CT, Ambrosio AMA, Borden MD, Cooper Jr. JA. Tissue engineering: orthopedic applications. Annu Rev Biomed Eng 1999;01:19.
19. Ma, Y., Liu, J., Luo, M., Xing, J., Wu, J., Pan, H., ... & Luo, Y. (2017). Incorporating isosorbide as the chain extender improves mechanical properties of linear biodegradable polyurethanes as potential bone regeneration materials. RSC Advances, 7(23), 13886-13895.
20. Lloyd, Andrew W. "Interfacial bioengineering to enhance surface biocompatibility." Medical device technology 13.1 (2002): 18-21.
21. Nair, Lakshmi S., and Cato T. Laurencin. "Biodegradable polymers as biomaterials." Progress in polymer science 32.8-9 (2007): 762-798.
22. Sabra, S., Ragab, D. M., Agwa, M. M., & Rohani, S. (2020). Recent advances in electrospun nanofibers for some biomedical applications. European Journal of Pharmaceutical Sciences, 144, 105224.
23. Samantaray, P. K., Little, A., Haddleton, D., McNally, T., Tan, B., Sun, Z., ... & Wan, C. (2020). Poly (glycolic acid)(PGA): a versatile building block expanding high performance and sustainable bioplastic applications. Green Chemistry.
24. Suzuki, A., & Shimizu, R. (2011). Biodegradable poly (glycolic acid) nanofiber prepared by CO2 laser supersonic drawing. Journal of Applied Polymer Science, 121(5), 3078-3084.
25. Dan, W., Chen, Y., Dan, N., Zheng, X., Wang, L., Yang, C., ... & Hu, Y. (2019). Multi-level collagen aggregates and their applications in biomedical applications. International Journal of Polymer Analysis and Characterization, 24(8), 667-683.
26. Minor, A. J., & Coulombe, K. L. (2020). Engineering a collagen matrix for cell-instructive regenerative angiogenesis. Journal of Biomedical Materials Research Part B: Applied Biomaterials.
27. Krishnamoorthy, G., Pugazhenthi, G., & Ramaiah, D. (2019). Resorbable polymer matrices: chitosan-substituted collagen-based biomaterials. In Materials for Biomedical Engineering (pp. 245-278). Elsevier.
28. Gu, L., Shan, T., Ma, Y. X., Tay, F. R., & Niu, L. (2019). Novel biomedical applications of crosslinked collagen. Trends in biotechnology, 37(5), 464-491.
29. Lin, K., Zhang, D., Macedo, M. H., Cui, W., Sarmento, B., & Shen, G. (2019). Advanced Collagen-Based Biomaterials for Regenerative Biomedicine. Advanced Functional Materials, 29(3), 1804943.
30. Hoerstrup, S. P., Zünd, G., Sodian, R., Schnell, A. M., Grünenfelder, J., & Turina, M. I. (2001). Tissue engineering of small caliber vascular grafts. European journal of cardio-thoracic surgery, 20(1), 164-169.

CHAPTER 2 Characterization and biocompatibility evaluation of artificial blood vessels prepared from pristine poly (Ethylene-glycol-co-1,4-cyclohexane dimethylene-co-isosorbide terephthalate), poly (1, 4 cyclohexane di-methylene-co-isosorbide terephthalate) nanofibers and their blended composition

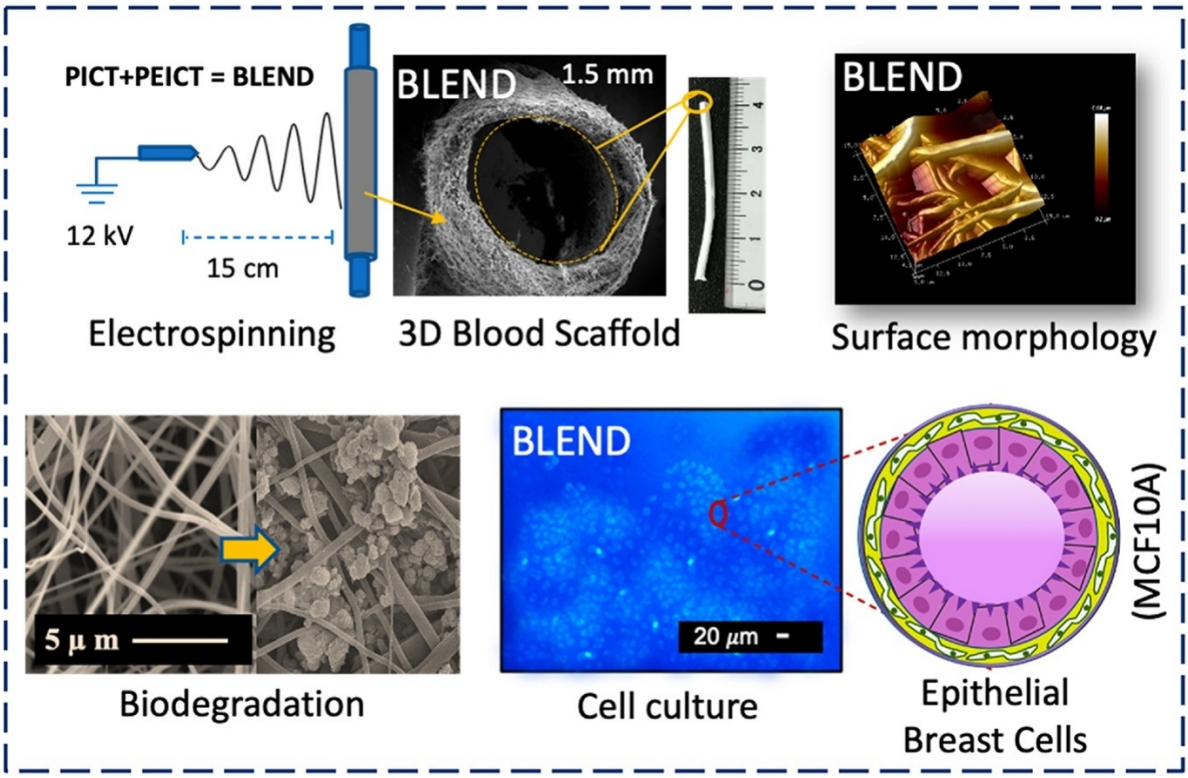

2.1. Introduction

The major problems related to heart bypass surgeries are conducted every year in the United States as approximatively 400,000 patients are diagnosed with cardiovascular diseases, mainly those related to vascular blockages [1,2].

At the present stage, artificial blood vessels (ABVs) with a cross-sectional diameter smaller than 2mm are not commercially available. On the other hand, autologous grafting is not appropriate for every patient [3].

Most of the naturally derived scaffolds have been of limited use due to their poor mechanical properties not allowing them to withstand the physiological pressure, simultaneously, they don't have sufficient biocompatible characteristics [4].

The surface properties are very important for an optimum cell growth and adhesion. Many pretreatments viz. plasma treatment, ozonation or ultraviolet treatments have been used to achieve the desired wettability, but they require a high energy consumption [5,6].

Considering all these issues, the challenge was to prepare smaller diameter ABVs with sufficient strength and good cell culture properties without using expensive and time-consuming surface treatments [6]. To avoid these processes, a blend of different substances with synchronized chemistry could provide an optimal surface for cell culture and adhesion [7]. Grafting is a conventional technique which has been utilized for vascular regeneration, but it is highly time consuming and requires double surgery [3,4,7].

Nanofibers represent promising characteristics such as higher surface area, diameter fineness, ease of three-dimensional fabrication, breathability and biocompatibility to fulfill the requirements of different functional applications viz. environmental, biomedical, smart wearables and tissue engineering [8–13].

Additionally, nanofibers show a morphological resemblance with the fibrillar components of the native Extra Cellular Matrix (ECM) and their unique physical characteristics make them suitable for engineering the tissue scaffolds of various types. These fibers provide a highly porous three-dimensional substrate making them able to mimic the native ECM, capable to interact with cells [14–16].

The potential applications of such nanofibers can be itemized as musculoskeletal tissues, namely cartilage, skin tissue, bone, ligament, tendon, vascular tissues and can be used as a carrier for drugs such as vitamins, DNAs and proteins [4,5,17]. Scaffolds having cell attachment, biocompatibility, biodegradability, non-immunogenicity and non-thrombogenicity properties can be considered to facilitate the regeneration of ABVs with a diameter less than 2mm of damaged tissues [11,17,18].

Bio-based polymers are considered as promising materials for the preparation of ABVs and other biomedical applications. Poly (1,4 cyclo-hexane di-methylene-co-isosorbide-terephthalate) (PICT) and Poly (Ethylene-glycol-co-1,4-cyclohexane di-methylene-co-isosorbide terephthalate) (PEICT) are naturally derived copolymers with considerable properties. They are originated from PCT, which has ductile mechanical properties and high glass transition temperature.

PICT is an eco-friendly co-polyester, containing the biomass Isosorbide, having very good mechanical properties [19], high glass transition temperature [20] and flexibility of 1,4-cyclohexanedimethanol (CHDM) cyclohexene ring [21]. Isosorbide, owing to its accessible synthesis has been considered as a preferred renewable monomer in terms of addressing environmental issues [22]. In parallel, it has good crystallinity [23], and thermal stability [24,25] and it has been potentially considered for various industrial, biomedical and textile applications [26].

PEICT has few different characteristics as another Isosorbide-based polyester that has been intensively explored due to its unique properties, such as high thermal resistance and biocompatible characteristics due to the presence of ethylene glycol [23].

Optimization of ABVs characteristics such as biocompatibility, tensile strength, ease of production, accessibility, viability and cell adhesion still remain a challenge as it is difficult to obtain all these properties from a single scaffold material. Thus, materials scientists are combining different polymers to make a suitable blend capable of overcoming the cell attachments problems of artificial scaffolds due to some physical and biological limitations such as fiber size, morphology and biocompatibility [27–29]. Human breast epithelial (MCF-10A) cells have been cultured and intensively utilized for the treatment and assessment of cancer disease [30] and different materials and medias for MCF-10A cell culture have been proposed for optimum cell growth [31].

Therefore, for the very first time we attempted to prepare nanofibrous ABVs with three different cross-sectional diameters 0.9, 1.5 and 2.0mm from pristine PICT, PEICT and their BLEND. The remained challenge was to prepare ABVs with a smaller diameter less than 2mm having sufficient mechanical and biocompatible properties at the same time. Pristine PICT, PEICT and their resultant BLEND were further characterized with respect of surface morphology, chemical structure, wettability and cell culture properties.

BLEND showed enhanced wettability, maximum cell adhesion and suitable nanofiber morphology for cell adhesion due to the change in surface properties which were distinctly imparted from PICT and PEICT. Interestingly, BLEND showed an additional novel feature of tunable tensile strength which was not observed in individual PICT or PEICT.

2.2. Experimental

2.2.1. Materials

Bio-based PEICT (Mw) (51,200 g/mol) and PICT (Mw) (46,800 g/mol) were obtained from SK Chemicals, Gyeonggido, Korea. As per literature, PEICT is composed of Ethylene glycol, Isosorbide, and CHDM with repeat units in 29.8, 22.7 and 47.2M ratios respectively. The chemicals present in PICT are Isosorbide and 1,4-cyclohexane dimethanol (CHDM) with repeating units in 11.1 and 88.9 M ratio respectively. Both PICT and PEICT copolymers were synthesized by melt condensation with various contents of the corn derived monomer Isosorbide. Terephthalic acid is used along with 1,4-cyclohexane di-methanol and the monomer Isosorbide. For obtaining the ester or PEICT oligomer, terephthalic acid was heated with the alcohol Ethylene Glycol and Isosorbide at 255°C followed by polycondensation at 270°C. Similarly, PICT copolyester was synthesized through esterification of TPA, ISB, and CHDM at 280°C, followed by a polycondensation process at 290°C. The only difference between PEICT and PICT lies in the presence of Ethylene Glycol in PEICT and a slight difference in the processing temperatures. The chemical composition of polymers has been confirmed by NMR in previous reports [21,23,32]. The chemical structures of PICT and PEICT can be seen in Scheme 1. Chloroform with 99% purity and Tri-fluoroacetic acid (TFA) with 98% purity were supplied by Wako Pure Chemical Industries, Ltd., Osaka, Japan. Phosphate buffered saline (PBS) and Dulbecco's modified Eagle's medium (DMEM) were supplied by Nacalai Tesque, Kyoto, Japan. EDTA was supplied by Merck (KGaA), Germany.

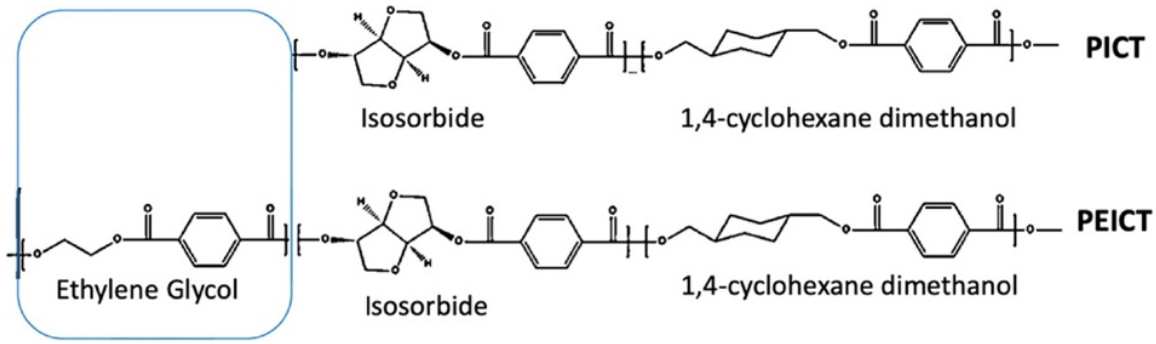

Scheme 2.1. Proposed chemical structures of PICT, PEICT and their BLEND

2.2.2. Preparation of PICT, PEICT and BLEND ABVs via electrospinning

10% (w/w) of each polymer (PICT and PEICT) solutions were prepared by dissolving the pellets individually in Chloroform/TFA (3:1). A transparent solution was formed when the pellets completely dissolved by stirring for two hours at room temperature. Polymer solution of the BLEND was prepared by mixing equal proportions of PICT and PEICT (1:1). All polymer solutions were separately placed in a syringe (5 ml), supplied with high voltage (13kV) using an electrospinning power supply (Har-100*12, Matsusada Co., Tokyo, Japan), maintaining the tip-collector distance of 15cm. The capillary tip (diameter of 0.8mm) was affixed with the syringe then placed on a syringe pump YSP-101 by YMC. The metallic rods of aluminum with diameters of 0.9, 1.5 and 2.0mm were used to prepare the three-dimensional ABVs. The electrospinning process was carried at room-temperature and 45–55% humidity. All nanofibrous ABV samples were immediately peeled off and dried in air prior to further characterizations [33].

2.3. Characterization

2.3.1. Biocompatibility evaluation (human breast cell culture)

MCF10A cell line was purchased from ATCC (ATCC CRL-10317). Cells were cultured in MEGM Bullet Kit media (Lonza, Singapore). All cell cultures were maintained in T25 flasks at temperature (37 ˚C) and CO2 content (5%), medium for culturing cells was replaced after a gap of 2 days. Nanofiber webs were cut into strips, UV treated for 30min before being placed into 6-well plates (Nunc^{TM}, ThermoFisher Scientific, Singapore). 500 uL of 8000 cells/ mL cells were added directly onto the fibers and maintained at 37˚C and 5% CO2. After 1h of allowing cell attachment, 2mL of media was added to the well. Following incubation conditions (37˚C and 5% of CO2) for 48h, the MCF10A cells were stained with 1ug/mL Hoechst 33342 (ThermoFisher Scientific, Singapore). Brightfield and UV images were taken to visualize cells that were still attached to the fibers. Normal microscope was not able to exhibit cells due to the opaque nanofiber surface, therefore, a fluorescence microscope was used to assess the cell culture by staining the nucleolus of MCF10A [34]. The average number of adhered cells on nanofibrous mats was manually calculated from 5 Fluorescence microscopic images from each sample type. The average MCF10A cell size of 15μm was taken as a reference for comparison.

2.3.2. Scanning electron microscopy (SEM)

The morphology of pristine PICT, PEICT and BLEND ABVs were examined using SEM (JSM-6010LA) by JEOL, Japan with accelerating voltage (10kV) and a maximum magnification of 5,000. PICT, PEICT and BLEND samples were initially coated with pb-pt for 120s using a fin coater (JFC-1200) from JEOL, Japan. The average diameter distribution of all nanofiber samples was measured using ImageJ software.

2.3.3. Atomic force microscopy (AFM)

AFM, Bruker, (Billerica, MA, USA) Dimension Icon was used to take AFM images of PICT, PEICT and BLEND nanofibers at room temperature using tapping cantilever (Bruker) due to irregular surfaces of nanofibers. A high-resolution Peak-Force imaging mode was used at 1 Hz to record the conditions. All topographic images were obtained under the same parameters such as retraction velocity (2μm/s), contact time (200ms) and the contact force (3nN). The resultant images were retuned using a software Nanoscope v1.7 [35].

2.3.4. Fourier transform infrared spectroscopy (FTIR)

The chemical composition of PICT and PEICT as well as the influence on the chemistry of BLEND ABVs were assessed using IR Prestige-21, Shimadzu (Kyoto, Japan) at ATR-FTIR mode. Adsorption spectra were assessed in the wavelength range ($650cm^{-1}$ to $4000cm^{-1}$) at room temperature.

2.3.5. Water contact angle (WCA) test

WCA tests for checking the wettability of PICT, PEICT and BLEND were carried on FACE model CA-VP, Kyowa interface science, Japan. WCA was assessed by measuring the static angle by drop testing method with drop of (2μl). 10 readings were taken from each sample for 300s.

2.3.6. Biodegradation of PICT, PEICT and BLEND nanofibers

PICT, PEICT and PICT/PEICT blend nanofibers underwent biodegradability tests with and without Porcine Pancreas Lipase (10mg) in 10mL of Phosphate Buffer Saline at PH 7.4 in form of incubation at 37°C with a continuous shaking (30rpm). The samples were checked every

four days. One sample from each type was thoroughly washed with ionized water, then dried in vacuum oven for 48h. The weight of the nanofiber samples before and after degradation was checked and the change in their morphology was assessed by SEM images, while the other samples had their buffer solution changed in order to maintain the enzymatic activity as well as the PH of PBS.

2.3.7. Tensile strength test

The tensile strength of PICT, PEICT and BLEND ABVs was checked by a Universal Tensile Tester (RTC 1250-A, A&D CO., Ltd., Tokyo, Japan). All the samples used had a thickness of 50±10μm and the same length. The tensile strength test was conducted using a load of 10N, a 30mm long gauge with the rate of extension (10mm/min). Error bars represent the uncertainties on the stress and strain values calculated from the standard deviation on the load measurement from three samples of each type of ABV.

2.4. Results and discussion

2.4.1. Optimization of bio-based nanofibers for cell culture

The human breast cell (MCF10A) growth is comparatively rapid than the other conventionally used cells, therefore breast cell-lines were chosen for checking the biocompatibility of PICT, PEICT and BLEND nanofibers [31]. Fig. 1(A) shows the cell culture on culture flask in 24h and 48h, the culture flask was fully covered with MCF10A in 48h [36].

Similarly, Fig. 1(B) shows the MCF10A cell culture on the surface of PICT, PEICT and BLEND nanofibers for 48h, BLEND showed very good cell adhesion of around 75%, PEICT showed a cells adhesion of about 22%. The probable reason to this may be the compactness and the smoother morphology of BLEND. Some MCF10A cells were attached on the surface of PEICT due to the difference in the average size of nanofiber diameter, compactness or other chemical differences which are discussed in section 4.4. On the other hand, no cells adhered on the surface of PICT, may be due to the bigger pore size of the surface of nanofibers which is revealed in the SEM images, the cells were transferred through the gaps between the PICT nanofibers may be due to the deeper pore size (AFM images) of nanofibers and the cells were alive in the flask placed below each nanofibers sample which were assessed under microscope during cell culture experiments. The results reveal that the presence of nanofibers does not resist the cell growth, thus PICT, PEICT and BLEND nanofibers are non-toxic and

biocompatible, and BLEND nanofibrous mat has the capability to hold more MCF10A cells on its surface compared to pristine PICT and PEICT. The probable reasons of this, may be a change in the surface morphology, chemical structure or wetting properties which are further confirmed by AFM, SEM, FTIR and water contact angle.

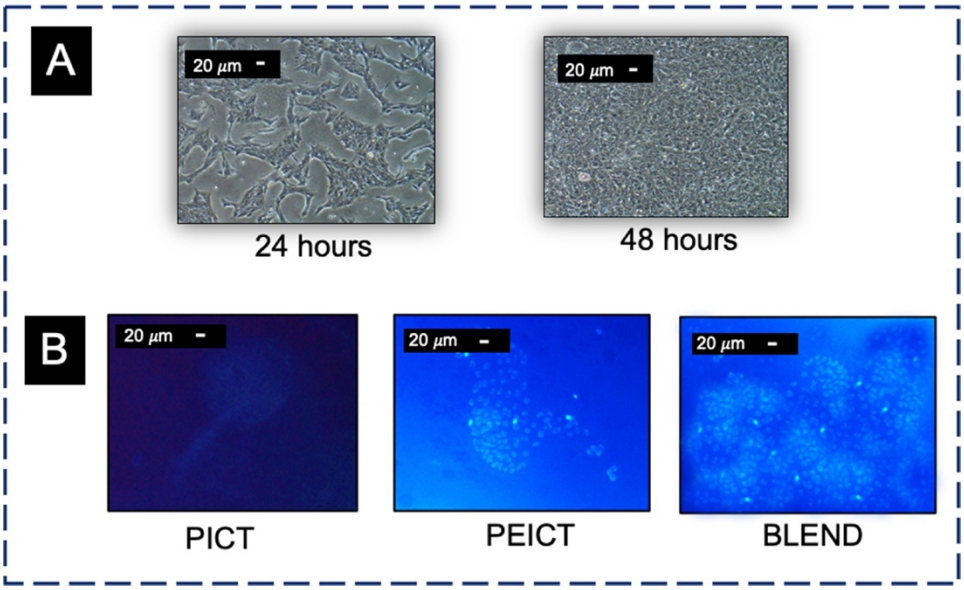

Fig. 2.1. (A) Microscopic images of MCF10A cell growth on culture flask, (B) Fluorescent microscopic images of MCF10A growth on surface of PICT, PEICT and BLEND nanofiber after 48 h.

2.4.2. Atomic force microscopy of PICT, PEICT and BLEND

To confirm the reason for the different behavior of cell attachment on different samples, it was an urge to check surface properties using AFM. Fig.2.2.(A, B and C) shows AFM images of PICT, PEICT and BLEND nanofiber surfaces respectively. The topographic images attained by AFM confirm that PICT nanofibers have finer diameters than PEICT supporting the data from SEM images of the nanofiber surfaces. More dents on the surface of PICT can be seen from AFM images and PEICT nanofibers show comparatively larger diameter with a slope-shaped tendency, whereas BLEND nanofibers show compacted surface with less dents compared to both PICT and PEICT nanofibers. AFM images also reveal the average dent depth histogram from the surface of each nanofiber sample as shown in Fig.2.2(D, E and F). PICT, PEICT and BLEND showed an average depth of (600±50nm), (700±40nm) and (450±20nm) respectively. BLEND showed a few major depths in the range of 700−800nm, maybe due to more random deposition of nanofibers during electrospinning. PEICT nanofibers showed comparatively bigger diameter size and a slide surface which were the reasons that only few MCF10A cells could adhere to its surface. Whereas, BLEND showed a small number of deep

dents with more compacted nanofibers on the surface having the potential to hold more MCF10A cells, which were difficult to be held on PICT (less-compactness) and PEICT (slide-shaped) nanofibers surfaces [37, 38].

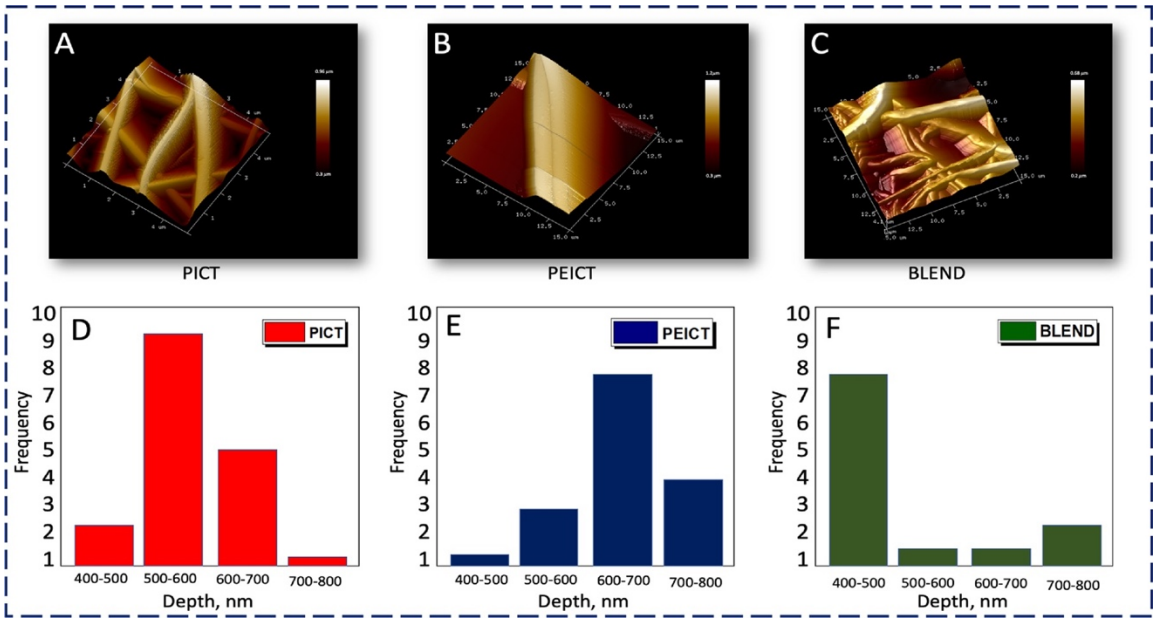

Fig. 2.2. AFM images of (A) PICT, (B) PEICT, (C) BLEND nanofiber surfaces and average depth histograms of (D) PICT, (E) PEICT, (F) BLEND nanofibers.

2.4.3. Morphology of PICT, PEICT and BLEND nanofiber scaffolds

Cross-sectional images and morphology of PICT, PEICT and BLEND ABVs are shown in Fig.2.3. These SEM illustrations demonstrate a smooth and regular morphology on both inner and outer surface of the ABVs which is beneficial for allowing an easy installation during surgical operations. The average wall thickness of PICT is 200±10µm and 500±10µm corresponds to that of PEICT and BLEND. The BLEND sample with 1.5mm diameter is observed to be smoother than pristine PICT and PEICT ABVs. Bead-free and smooth morphology of PICT, PEICT and BLEND nanofibers are revealed in Fig.2.4.A, B and C respectively, confirming that the blending of PICT and PEICT does not exert any negative influence on the morphology of the resultant nanofiber BLEND. Fig.2.4. D, E and F demonstrate the average diameter distributions of PICT with (300±40nm), PEICT with (600±80nm) and BLEND with (350±50nm) respectively. Ultimately, BLEND nanofibers are considerably finer than PEICT and their average diameter tends towards the morphology of PICT nanofibers. Ultimately, the difference in the diameter of nanofibers reveals its effect on cell infiltration which has previously been discussed in cell culture section.

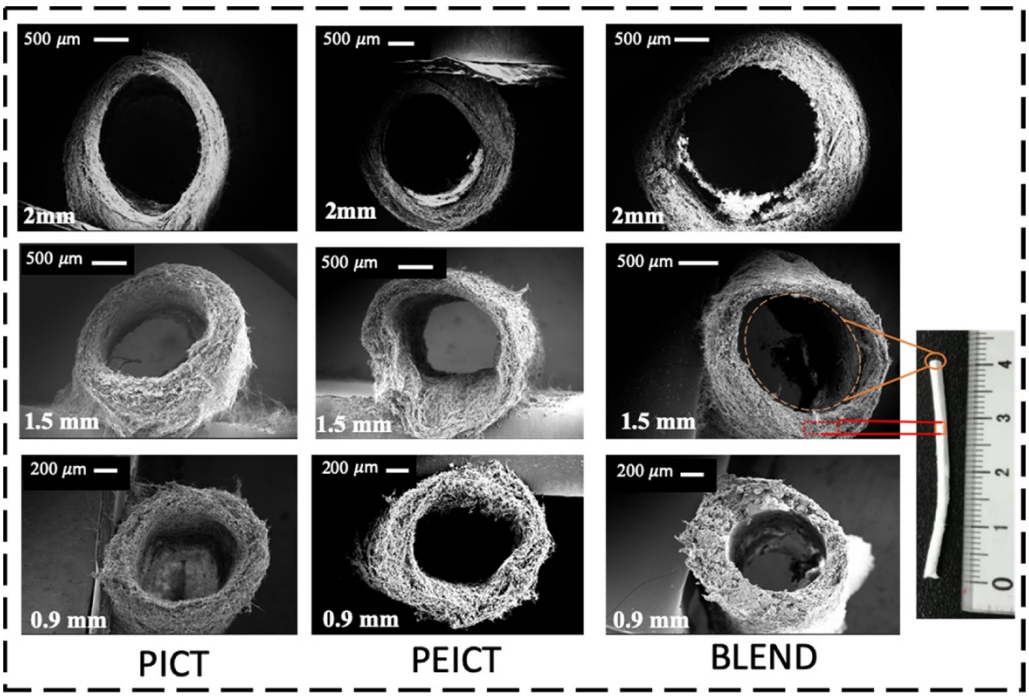

Fig. 2.3. Photographic images of ABVs of PICT, PEICT and BLEND nanofibers with three cross-sectional diameters 0.9, 1.5 and 2.0 mm for each type.

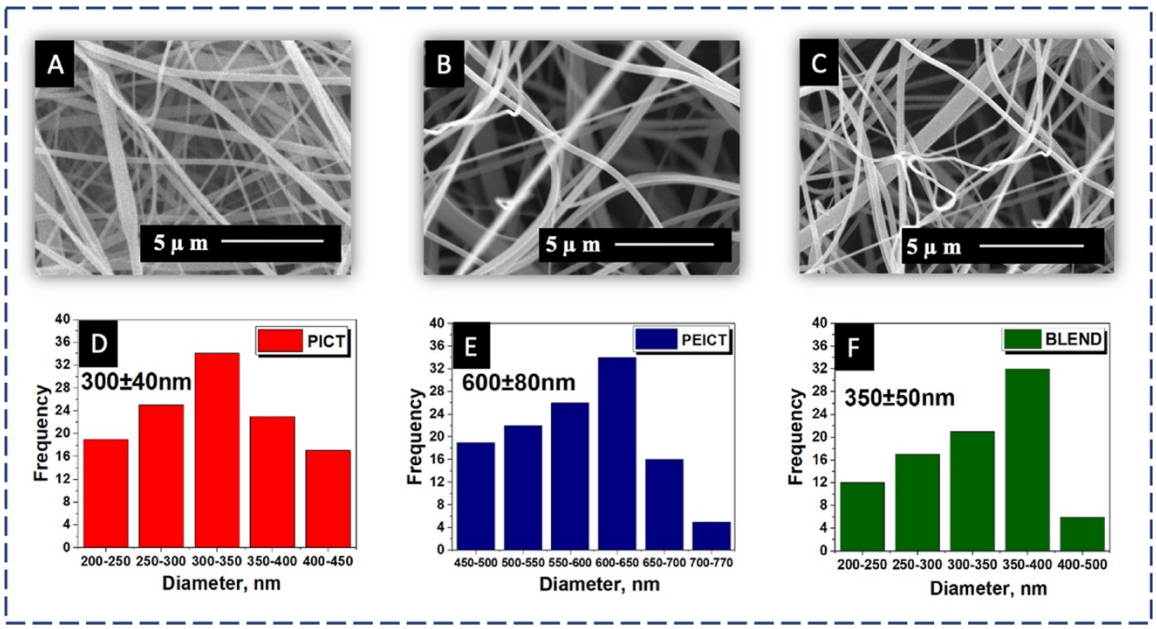

Fig. 2.4. SEM images of (A) PICT, (B) PEICT, (C) BLEND and Diameter distribution graphs of (D) PICT, (E) PEICT, (F) BLEND nanofibers.

2.4.4. Chemical structure of PICT, PEICT and BLEND nanofibers (FTIR)

Fig.2.5 shows the main characteristic peaks of PICT, PEICT and their BLEND nanofibers. The main difference in the chemical structure of PEICT and PICT was the presence and absence of Ethylene Glycol (EG) respectively in their chemical composition, due to the peaks appearing at 1244cm^{-1} (cis- comparatively intensive for PEICT) and 1264cm^{-1} (trans-comparatively intensive for PICT) [23–35]. Usually this chemical part (-COOH) plays a leading role in the biodegradation of polyesters when attacked by porcine pancreases lipase [39]. Interestingly, BLEND showed more intensive peaks at all the characteristic points, because of good intimate blending between PICT and PEICT. Significantly, the spectrum at 726cm^{-1} reveals CH, 1094cm^{-1} reveals CN, 1715cm^{-1} shows C=O and 2854cm^{-1} represents CH group. The peaks 2925cm^{-1} and 2930cm^{-1} indicate CH present in PICT and PEICT respectively, whereas in BLEND, the peaks of CH split the same range of the FTIR spectrum and appeared as two small peaks at 2924cm^{-1} and 2930cm^{-1} which reveals more CH groups present in BLEND compared to pristine PICT and PEICT [40,41]. The results confirmed that the chemical structures of PICT and PEICT were distinctly imparted to BLEND nanofiber sample with more functional groups (-CH) on its surface, this may also be the reason for more cell adhesion on BLEND which may result in enhanced wettability on BLEND nanofibers due to the change in chemical properties as an ultimate reason of better cell attachment [40,44].

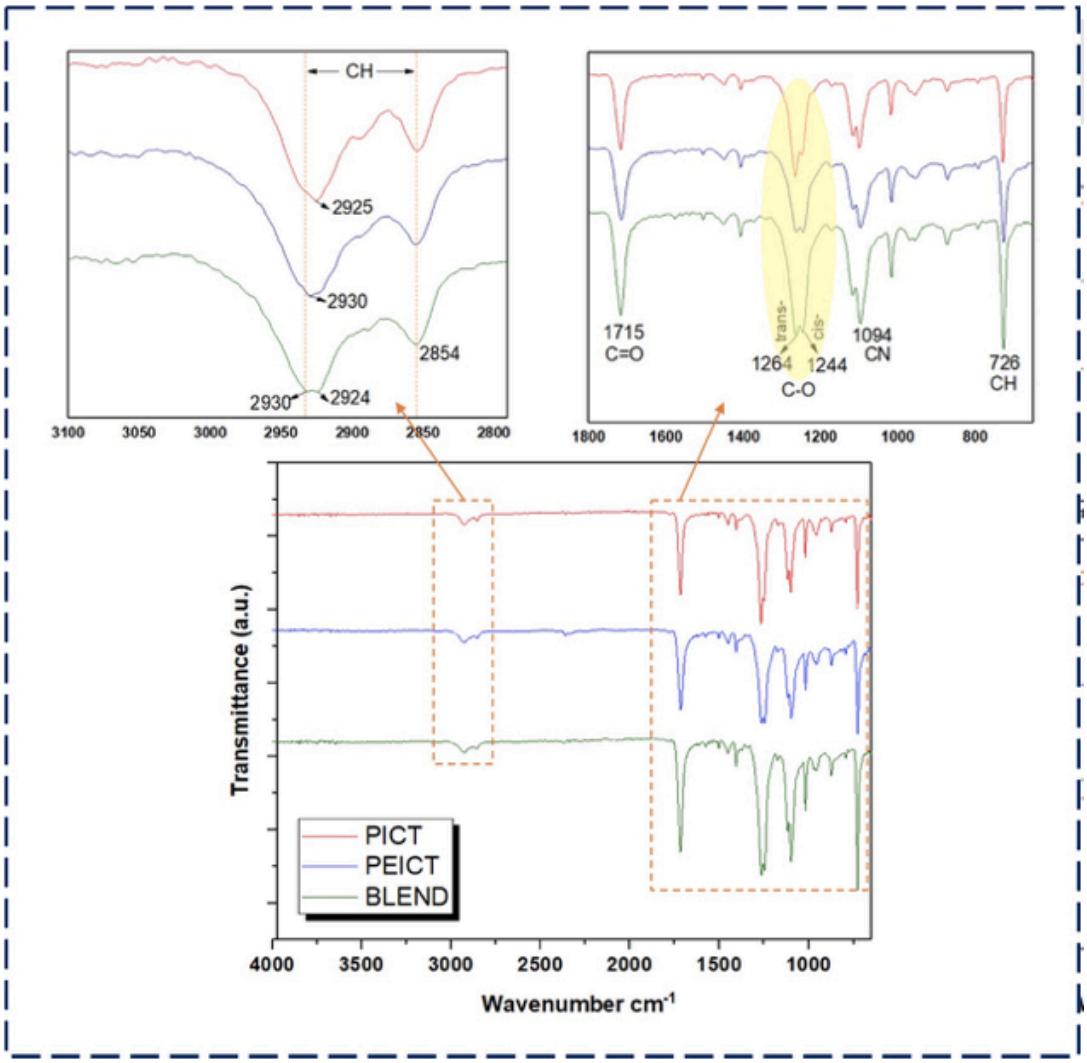

Fig. 2.5. FTIR spectra of PICT, PEICT and BLEND ABVs.

2.4.5. Wettability of PICT, PEICT and BLEND nanofibers

WCA of pristine PICT, PEICT and their BLEND is demonstrated in Fig.2.6. All nanofiber samples were observed as hydrophobic. The WCA of PICT was observed as maximum with 124°±2°, PEICT showed less hydrophobicity than PICT with WCA 114°±3° due to the presence of Ethylene Glycol containing -OH groups in the molecular composition of PEICT, whereas BLEND showed minimum hydrophobic character compared to pristine PICT and PEICT. Surfaces with less hydrophobicity are more likely to adhere cells [40–44], probably due to this higher wettability of BLEND, more cells could adhere on BLEND compared to pristine PICT or PEICT nanofiber mats [45–47]. The wettability of BLEND surfaces was increased due to the increased number of Hydrogens in the form of -CH, -COOH groups imparted from both PICT and PEICT along with the presence of Ethylene Glycol in the form

of -OH groups in the molecular structure of PEICT on its surface as confirmed by FTIR. Another reason of the increased wettability was the smoother surface as revealed per AFM topographic images of nanofiber samples. Wettability of BLEND nanofiber surface increased without incorporation of any additional chemicals or any special pretreatments [7,45].

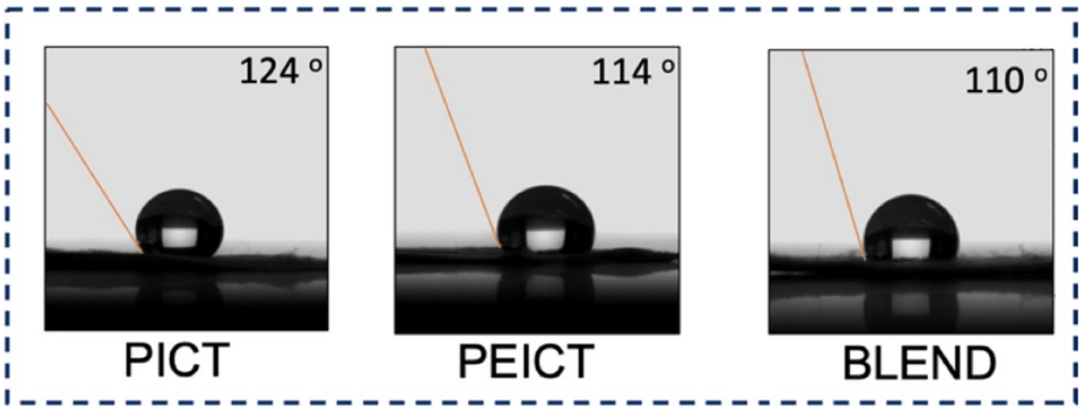

Fig. 2.6. WCA test of PICT, PEICT and BLEND nanofibers.

2.4.6. Biodegradation of PICT, PEICT and BLEND

Enhanced wettability and increased functional groups on the surface of BLEND nanofibers inspired this research for the assessment of biodegradation of all samples. The biodegradation characteristics of PICT, PEICT and BLEND was assessed with respect to mass degradation (weight loss %) and enzymatic degradation of nanofibers over the time as shown in Fig.2.7.

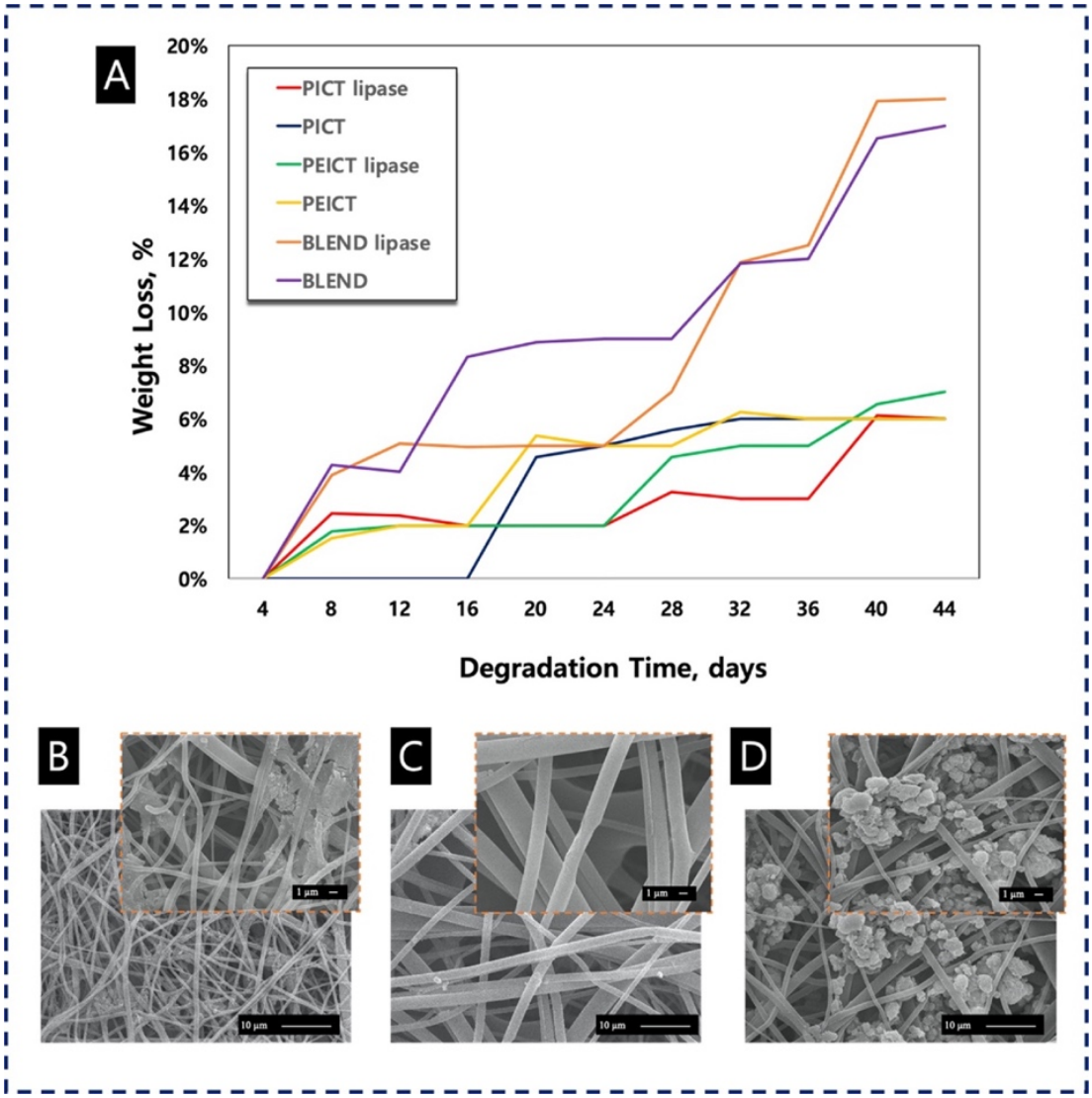

Fig. 2.7. (A) Mass Degradation of PICT, PEICT and BLEND and Morpho-degradation of (B) PICT, (C) PEICT, (D) BLEND.

Fig.2.7(A) exhibits that PICT showed 6% weight loss in 44 days without influence of Lipase. Initially, a slow degradation rate was observed but the degradation rate increased with the time. PEICT nanofibers showed 7% weight loss with lipase having a slow degradation rate until 20 days and later a rapid degradation rate was observed, maybe because of Ethylene Glycol present in its chemical structure, where 6% of the weight loss occurred without Lipase until 44 days. BLEND nanofibers showed a maximum weight loss of 18% after 44 days when placed with Lipase in PBS. Until 30 days, a slower degradation rate was observed due to the initial interaction of lipase with the functional groups, later the degradation rate increased due to the bulk release of Ethylene Glycol because of the higher surface area of BLEND nanofibers, the pH increased to slightly alkaline medium where a lipase could perform comparatively better degradation and reached 18%. BLEND showed interesting results when checked without lipase,

a weight loss of 17% was observed with a consistent degradation rate. Maximum degradation of BLEND occurred because of more functional groups (-COOH and -OH) on its surface which were distinctly imparted from PICT and PEICT [39]. Compared to pristine PICT and PEICT, their BLEND showed higher degradation properties which can be set as consistent or intermittent by using or not using porcine pancreas lipase respectively.

2.4.7. Mechanical properties of PICT, PEICT and BLEND ABVs

Fig.2.8 reveals the tensile strength graphs of ABVs with respect to the polymer type and the vessels inner diameter. The tensile strength graphs of PICT ABVs of three different cross-sectional diameters are shown in Fig.2.8(A), the ABV with 2.0mm diameter showed the maximum stress 5.10MPa, and the maximum strain 22.5mm was observed in the ABV with 0.9mm diameter and a stress of 4.71MPa, whereas the ABV of 1.5 mm diameter showed intermediate results between ABVs of 2.0mm and 0.9mm diameter with a stress of 4.59MPa and a strain of 7.85mm. Fig.2.8(B) demonstrates the tensile properties of PEICT nanofibrous ABV. The tensile strength of the ABV at 2.0mm diameter showed maximum stress of 5.01MPa and a strain of 52.33mm. The maximum strain was observed at the 1.5mm diameter ABV as 54.88 mm whereas the 0.9mm diameter ABV revealed minimum stress/strain values compared to PEICT ABVs of 2.0mm and 1.5mm diameter.

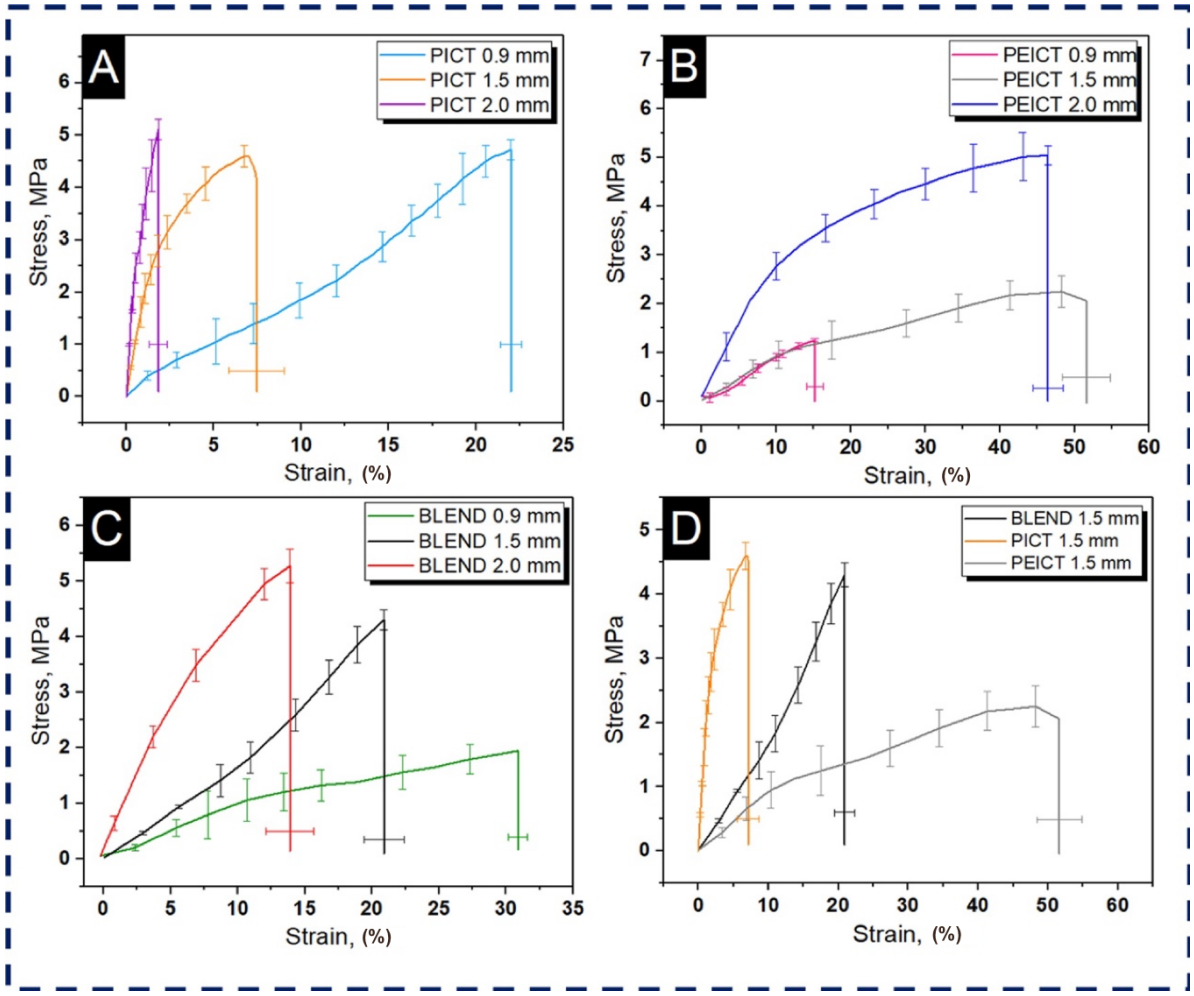

Fig. 2.8. Tensile strength of (A) PICT, (B) PEICT, (C) BLEND ABVs with respect to diameters (0.9, 1.5 and 2.0 mm) and (D) A comparison between tensile strength of PICT, PEICT and BLEND ABVs at 1.5 mm diameter.

The tensile strength graphs of BLEND ABVs with respect to different diameters are shown in Fig.2.8(C). The results showed a specific relationship which can be tuned by increasing and decreasing the diameter of the BLEND ABVs, adding value to the BLEND ABVs to be used with optimized mechanical properties [44,46], which could not be observed in the tensile properties of pristine PICT and PEICT. In BLEND ABVs, increasing diameter of ABVs results in increasing stress values, in fact, the maximum stress (5.2MPa) is attained in the 2.0mm diameter sample, ABV with 1.5mm diameter shows a stress of 4.3MPa, and the ABV with 0.9 diameter revealed the stress of 1.94MPa. Interestingly, another relation is observed in BLEND ABVs, stress-strain graph concerns the decreasing the BLEND ABVs diameter that leads to increasing their strain. In fact, the 0.9mm diameter samples showed a maximum strain of 31.65mm, while the 1.5mm diameter ABVs showed 21.37mm and the ABVs of 2.0mm diameter showed a strain of 14.44mm. Fig.2.8(D) shows a comparison between the tensile

strength of 1.5mm diameter PICT, PEICT and BLEND ABVs, since this specific diameter has attained optimum intermediate results in all types of ABVs in this report. PICT nanofibrous ABVs showed a maximum stress of 4.60MPa and PEICT showed a maximum strain of 54.88mm, whereas BLEND ABVs showed intermediate tensile properties between PICT and PEICT ABVs with stress and strain values of 4.3MPa and 21.37mm respectively. The ratio of PICT ABVs may result in increased stress and the ratio of PEICT ABVs may result in an increased strain of the BLEND ABVs. The reasons behind different tensile strength may be the difference in average diameter of nanofibers or the chemical composition of each sample. These results confirmed that the tensile strength of BLEND is more suitable for the preparation of ABVs which depends on either increasing or decreasing their cross-sectional diameters, and this tunable tensile strength property could be observed only in BLEND ABVs and does not apply for pristine PICT or PEICT ABVs [48].

2.5. Conclusion

Three different types of ABVs with three cross-sectional diameters (0.9mm, 1.5mm and 2.0mm) from pristine PICT, PEICT and their BLEND with ratio (1:1) were successfully prepared using an adapted electrospinning setup. Biocompatibility of all samples was confirmed by culturing MCF10A cells. BLEND showed very good cell adhesion of about 75%, PEICT showed a cell adhesion of about 22% while no cells were found on the surface of PICT nanofibers. This was due to the more compacted and smoother morphology of BLEND nanofibers, leading to smaller gaps between nanofibers surface as revealed by AFM images. Collective chemical and mechanical properties of PICT and PEICT were distinctly imparted into BLEND ABVs. More functional groups on the BLEND surface resulted in an enhanced wettability of BLEND. SEM images revealed smooth morphology of all nanofibers before biodegradation, whereas BLEND (300±40nm) showed around 50nm bigger diameter than PICT (350±50nm) and PEICT nanofibers (600±80 nm) showed 250nm bigger average diameter than BLEND nanofibers. Maximum biodegradation was observed in BLEND nanofibers without any significant influence of the presence of Lipase. The resultant ABVs demonstrated a linear change in tensile strength properties by tuning the cross-sectional diameter, which does not work for pristine PICT and PEICT ABVs. BLEND showed optimum tensile properties for the ABV with 1.5mm cross-sectional diameter, which could bear the stress of 5MPa with 21% of strain. The results confirmed that all attributes of BLEND nanofibers make them suitable to be considered for vascular regeneration and cell culture applications.

2.6. References

1. M. Kivima ̈ki, A. Steptoe, Effects of stress on the development and progression of cardiovascular disease, Nat. Rev. Cardiol. 15 (4) (2018) 215.
2. J. Zhang, L.F. Chu, Z. Hou, M.P. Schwartz, T. Hacker, V. Vickerman, et al., Functional characterization of human pluripotent stem cell-derived arterial endothelial cells, Proc. Natl. Acad. Sci. 114 (30) (2017) E6072–E6078.
3. M.R. De Vries, K.H. Simons, J.W. Jukema, J. Braun, P.H. Quax, Vein graft failure: from pathophysiology to clinical outcomes, Nat. Rev. Cardiol. 13 (8) (2016) 451.
4. Z. Syedain, J. Reimer, M. Lahti, J. Berry, S. Johnson, R. Bianco, R.T. Tranquillo, Tissue engineering of acellular vascular grafts capable of somatic growth in young lambs, Nat. Commun. 7 (1) (2016) 1–10.
5. S. Lanzalaco, L.J. Del Valle, P. Turon, C. Weis, F. Estrany, C. Alem ́an, E. Armelin, Polypropylene mesh for hernia repair with controllable cell adhesion/de-adhesion properties, J. Mater. Chem. B (2020).
6. R. Toita, K. Tsuru, K. Ishikawa, Ozone-gas-mediated surface hydrophilization enhances the cell responses to titanium, Mater. Lett. 261 (2020), 127168.
7. D. Park, E. Wershof, S. Boeing, A. Labernadie, R.P. Jenkins, S. George, et al., Extracellular matrix anisotropy is determined by TFAP2C-dependent regulation of cell collisions, Nat. Mater. 19 (2) (2020) 227–238.
8. U.A. Qureshi, Z. Khatri, F. Ahmed, M. Khatri, I.S. Kim, Electrospun zein nano ber as a green and recyclable adsorbent for the removal of reactive black 5 from the aqueous phase, ACS Sustain. Chem. Eng. 5 (5) (2017) 4340–4351.
9. M.Khatri,F.Ahmed,A.W.Jatoi,R.B.Mahar,Z.Khatri,I.S.Kim,Ultrasonicdyeing of cellulose nano bers, Ultrason. Sonochem. 31 (2016) 350–354.
10. M. Khatri, F. Ahmed, I. Shaikh, D.N. Phan, Q. Khan, Z. Khatri, et al., Dyeing and characterization of regenerated cellulose nano bers with vat dyes, Carbohydr. Polym. 174 (2017) 443–449.
11. W.J.Zhang,W.Liu,L.Cui,Y.Cao,Tissueengineeringofbloodvessel,J.Cell.Mol. Med. 11 (5) (2007) 945–957.
12. P. Feng, P. Wu, C. Gao, Y. Yang, W. Guo, W. Yang, C. Shuai, A multi-material scaffold with tunable properties: toward bone tissue repair, Adv. Sci. 5 (6) (2018) 1700817.
13. C. Gualandi, M. Govoni, L. Foroni, S. Valente, M. Bianchi, E. Giordano, et al., Ethanol disinfection affects physical properties and cell response of electrospun poly (l-lactic acid) scaffolds, Eur. Polym. J. 48 (12) (2012) 2008–2018.
14. L. Wang, S. Xie, Z. Wang, F. Liu, Y. Yang, C. Tang, et al., Functionalized helical bre bundles of carbon nanotubes as electrochemical sensors for long-term in vivo monitoring of multiple disease biomarkers, Nat. Biomed. Eng. 4 (2) (2020) 159–171.
15. A. Restuccia, D.T. Seroski, K.L. Kelley, C.S. O'Bryan, J.J. Kurian, K.R. Knox, et al., Hierarchical self-assembly and emergent function of densely glycosylated peptide nano bers, Commun. Chem. 2 (1) (2019) 1–12.
16. E.A. Cavalcanti-Adam, Building nanobridges for cell adhesion, Nat. Mater. 18 (12) (2019) 1272–1273.
17. D. Radke, W. Jia, D. Sharma, K. Fena, G. Wang, J. Goldman, F. Zhao, Tissue engineering at the blood-contacting surface: a review of challenges and strategies in vascular graft development, Adv. Healthc. Mater. 7 (15) (2018) 1701461.
18. S. Kaushal, G.E. Amiel, K.J. Guleserian, O.M. Shapira, T. Perry, F.W. Sutherland, et al., Functional small-diameter neovessels created using endothelial progenitor cells expanded ex vivo, Nat. Med. 7 (9) (2001) 1035–1040.

19. S. Legrand, N. Jacquel, H. Amedro, R. Saint-Loup, J.P. Pascault, A. Rousseau, F. Fenouillot, Synthesis and properties of poly (1, 4-cyclohexanedimethylene-co-isosorbide terephthalate), a biobased copolyester with high performances, Eur. Polym. J. 115 (2019) 22–29.
20. Y.G. Jeong, W.H. Jo, S.C. Lee, Cocrystallization of Poly (1, 4-cyclohexylenedi- methylene terephthalate-co-hexamethylene terephthalate) Copolymers, Macromol. Res. 12 (5) (2004) 459–465.
21. J.M. Koo, S.Y. Hwang, W.J. Yoon, Structural and thermal properties of PCT containing isosorbide, Polym. Chem. 6 (2015) 6973–6986.
22. Y.Ma,J.Liu,M.Luo,J.Xing,J.Wu,H.Pan,etal.,Incorporatingisosorbideasthe chain extender improves mechanical properties of linear biodegradable polyurethanes as potential bone regeneration materials, RSC Adv. 7 (23) (2017) 13886–13895.
23. D.N. Phan, H. Lee, D. Choi, C.-Y. Kang, S.S. Im, I.S. Kim, Fabrication of two polyester nano ber types containing the biobased monomer isosorbide: poly (ethylene glycol 1,4-cyclohexanedimethylene isosorbide terephthalate) and poly (1,4-cyclohexanedimethylene isosorbide terephthalate), Nanomaterials 8 (2018) (2018) 56.
24. M.Q. Khan, H. Lee, Z. Khatri, D. Kharaghani, M. Khatri, T. Ishikawa, S. S. Im, I. S. Kim, Fabrication and characterization of nano bers of honey/poly (1, 4-cyclohexane dimethylene isosorbide trephthalate) by electrospinning. Materials Science and Engineering: C, 81, 247-251.
25. A.F. Naves, H.T. Fernandes, A.P. Immich, Enzymatic syntheses of unsaturated polyesters based on isosorbide and isomannide, J. Polym. Sci. Part A: Polym. Chem. 51 (18) (2013) 3881–3891.
26. M.Q. Khan, H. Lee, J.M. Koo, Z. Khatri, J. Sui, S.S. Im, et al., Self-cleaning effect of electrospun poly (1, 4-cyclohexanedimethylene isosorbide terephthalate) nano bers embedded with zinc oxide nanoparticles, Text. Res. J. 88 (2018) 2493–2498.
27. Y. Nakayama, W. Yagumo, R. Tanaka, T. Shiono, K. Inumaru, C. Tsutsumi, et al., Synthesis, properties and biodegradation of periodic copolyesters composed of hydroxy acids, ethylene glycol, and terephthalic acid, Polym. Degrad. Stab. 174 (2020) 109095.
28. D.K. Zhang, A.S. Cheung, D.J. Mooney, Activation and expansion of human T cells using arti cial antigen-presenting cell scaffolds, Nat. Protoc. (2020) 1–26.
29. D. Wang, Y. Xu, Q. Li, L.S. Turng, Arti cial small-diameter blood vessels: materials, fabrication, surface modi cation, mechanical properties, and bioactive functionalities, J. Mater. Chem. B 8 (9) (2020) 1801–1822.
30. B. Yang, H. Wolfenson, V.Y. Chung, et al., Stopping transformed cancer cell growth by rigidity sensing, Nat. Mater. (2020) 239–250.
31. Wei Huang, Lin Zhu, Chao Zhao, Xiangfeng Chen, Zongwei Cai, Integration of proteomics and metabolomics reveals promotion of proliferation by exposure of bisphenol S in human breast epithelial MCF-10A cells, Sci. Total Environ. (2020) 136453.
32. J.W. Yoon, S.Y. Hwang, J.M. Koo, Y.J. Lee, S.U. Lee, S.S. Im, Synthesis and characteristics of a biobased high-tg terpolyester of isosorbide, ethylene glycol, and 1,4-Cyclohexane dimethanol: effect of ethylene glycol as a chain Linker on polymerization, Macromolecules 46 (2013) 7219–7231.
33. Z. Khatri, A.W. Jatoi, F. Ahmed, I.S. Kim, Cell adhesion behavior of poly (ε-caprolactone)/poly (L-lactic acid) nano bers scaffold, Mater. Lett. 171 (2016).
34. N. Udomluck, H. Lee, S. Hong, S.H. Lee, H. Park, Surface functionalization of dual growth factor on hydroxyapatite-coated nano bers for bone tissue engineering, Appl. Surf. Sci. (2020) 146311.
35. Y. Gao, L. Yu, J.C. Yeo, C.T. Lim, Flexible hybrid sensors for health monitoring: materials and mechanisms to render wearability, Adv. Mater. (2019) 1902133.

36. T.L. Nguyen, E.R. Polanco, A.N. Patananan, et al., Cell viscoelasticity is linked to fluctuations in cell biomass distributions, Sci. Rep. 7403 (2020).
37. K. Wu, X. Zhang, W. Yang, X. Liu, Y. Jiao, C. Zhou, Imfluence of layer-by-layer assembled electrospun poly (l-lactic acid) nanofiber mats on the bioactivity of
38. X. Dong, X. Yuan, L. Wang, J. Liu, A.C. Midgley, Z. Wang, et al., Construction of a bilayered vascular graft with smooth internal surface for improved hemocompatibility and endothelial cell monolayer formation, Biomaterials 181 (2018) 1–14.
39. Jincheng Tang, Zheguo Zhang, Zifeng Song, Liran Chen, Xin Hou, Yao. Kangde, Synthesis and characterization of elastic aliphatic polyesters from sebacic acid, glycol and glycerol, Eur. Polym. J. 42 (12) (2006) 3360–3366.
40. Y. Arima, H. Iwata, Effect of wettability and surface functional groups on protein adsorption and cell adhesion using well-defined mixed self-assembled monolayers, Biomaterials 28 (20) (2007) 3074–3082.
41. C. Shuai, L. Yu, P. Feng, Y. Zhong, Z. Zhao, Z. Chen, W. Yang, Organic montmorillonite produced an interlayer locking effect in a polymer scaffold to enhance interfacial bonding, Mater. Chem. Front. 4 (8) (2020) 2398–2408.
42. M.C. Arno, M. Inam, A.C. Weems, et al., Exploiting the role of nanoparticle shape in enhancing hydrogel adhesive and mechanical properties, Nat. Community. 1420 (2020).
43. S. Rahimipour, E. Salahinejad, E. Shari , H. Nosrati, L. Tayebi, Structure, wettability, corrosion and biocompatibility of nitinol treated by alkaline hydrothermal and hydrophobic functionalization for cardiovascular applications, Appl. Surf. Sci. 506 (2020), 144657.
44. X. Xun, Y. Wan, Q. Zhang, D. Gan, J. Hu, H. Luo, Low adhesion superhydrophobic AZ31B magnesium alloy surface with corrosion resistant and anti-bioadhesion properties, Appl. Surf. Sci. 505 (2020), 144566.
45. X. Zhang, P. Xu, M. Zhang, G. Liu, Z. Xu, J. Yang, et al., Improving the wettability of Ag/ZrB2 system by Ti, Zr and Hf addition: an insight from first-principle calculations, Appl. Surf. Sci. (2020) 146201.
46. J.P. Luo, Y.J. Huang, J.Y. Xu, J.F. Sun, M.S. Dargusch, C.H. Hou, et al., Additively manufactured biomedical Ti-Nb-Ta-Zr lattices with tunable Young's modulus: mechanical property, biocompatibility, and proteomics analysis, Mater. Sci. Eng. C (2020) 110903
47. P. Feng, Y. Kong, L. Yu, Y. Li, C. Gao, S. Peng, et al., Molybdenum disulfide nanosheets embedded with nanodiamond particles: co-dispersion nanostructures as reinforcements for polymer scaffolds, Appl. Mater. Today 17 (2019) 216–226,
48. H. Lee, J.M. Koo, D. Sohn, I.S. Kim, S.S. Im, High thermal stability and high tensile strength terpolyester nanfibers containing biobased monomer: fabrication and characterization, RSC Adv. 6 (46) (2016) 40383–40388.

CHAPTER 3 Fabrication of Poly(Ethylene-glycol 1,4-Cyclohexane Dimethylene-Isosorbide-Terephthalate) Electrospun Nanofiber Mats for Potential Infiltration of Fibroblast Cells

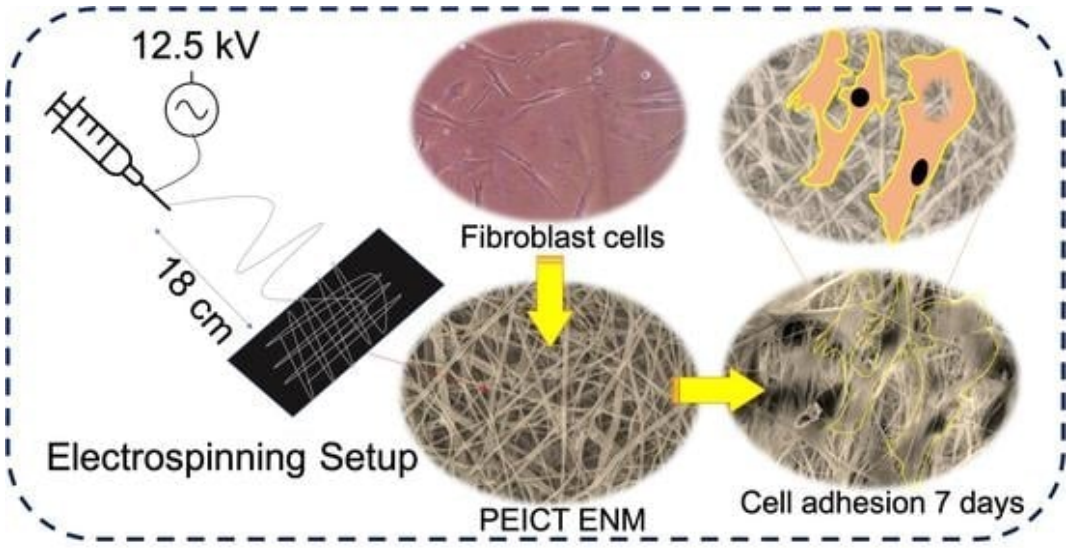

3.1. Introduction

Recently, bio-based polyesters have been widely studied for biomedical applications such as cell culture, drug delivery, and wound dressing [1–6]. Scientists have started exploring the biomedical applications of Isosorbide-based polyesters by virtue of their high tensile strength and good thermal stability [4,6–9]. Electrospun nanofiber mats (ENMs), due to their high surface area, ease of production, fiber network interconnection, biocompatibility, breathability, and resemblance to natural extracellular matrix have been potentially considered for cell culture applications viz. cell adhesion, cell migration, and cell viability [10–13]. In parallel, ENMs have been utilized in several applications including sensors [14], wound dressing [10], drug delivery [5], tissue engineering [15], smart apparels [16,17], high performance filters (water, bacteria, virus, heavy metal, and such impurities) [18–21]. Depending on the required application, cell adhesion and cell migration behaviors may differ due to the difference in cell size, type, or the culturing surface [4,6]. Scaffolds based on ENMs possess good biodegradability, biocompatibility, non-thrombogenicity, and non-immunogenicity, however, the optimization of such materials is challenging in terms of cell viability, cell infiltration, cell adhesion, and migration properties [4–6,10,11,22].

Poly(ethylene-glycol 1,4-cyclohexane dimethylene-isosorbide-terephthalate) (PEICT) ENMs, in light of their high glass transition temperature [23], good mechanical properties [8],

flexibility [6], thermal stability [4] and good crystallinity [23] have been potentially studied for various biomedical applications [4,6].

In our previous report, we investigated pristine poly(1,4-cyclohexane di-methylene-isosorbide-terephthalate) (PICT), PEICT, and their blended composition. We observed that no sufficient cell infiltration could be achieved due to the unsuitable nanofiber network on the surface, which could not hold breast epithelial cells on the surface of PEICT ENMs [4], therefore, we tried to explore the potential of PEICT ENMs for cell culture applications and to check the effect of surface properties of PEICT ENMs whether they allow fibroblast cell infiltration [4]. Fibroblast cells have been used to check the biocompatibility, cell infiltration, cell adhesion, and cell viability of different polymeric materials [6,13].

To serve the main purpose of this research, Isosorbide bio-based PEICT ENMs were prepared via electrospinning and used as a fibroblast cell permeable layer for the first time. There are few reports that have discussed the chemical structure of PEICT only characterized by FTIR spectroscopy, while in this report, the chemical structure of PEICT ENMs was significantly explored by x-ray photoelectron spectroscopy (XPS) validated by the FTIR results [4,8,23].

The wettability of PEICT ENMs was checked by the WCA test with respect to time as one of the important factors for cell adhesion to optimize the initial resting of fibroblast cells on PEICT ENMs. The nanofiber network and surface topography of PEICT ENMs were studied with respect to fibroblast cell infiltration. The results revealed the potential of PEICT ENM to be used as a biomaterial for fibroblast cell culture.

3.2. Materials and Methods

3.2.1. Materials

The polymer PEICT with an average molecular weight of 46,800 (g/mol) was supplied by SK Chemicals, Gyeonggi-do, Korea [8]. Chloroform (99%), and trifluoroacetic acid (TFA) (98%) were purchased from Wako, Pure Chemical Industries Ltd., Osaka, Japan. Ethanol (99.8%) was obtained by Merck, Japan. Cell migration on PEICT ENMs was performed using NIH 3T3 mouse fibroblast obtained from ATCC (Manassas, VA), USA [24]. The 24-well cell culture flasks and Petri-dishes were obtained from SPL Life Sciences (Pocheon, Korea). Ethylenediaminetetraacetic acid (EDTA) was purchased from Merck (KGaA), Germany.

Dulbecco's modified Eagle's medium (DMEM) was supplied by Nacalai Tesque, Kyoto, Japan. Fetal bovine serum (FBS) and Dulbecco's phosphate-buffered saline (DPBS) were provided by HyClone (Logan, UT, USA). The Cell Counting Kit-8 (CCK-8) reagent was obtained from Dojindo Laboratories Japan [25].

3.2.2. Preparation of PEICT ENM

A total of 11% (*w*/*w*) of PEICT solution was stirred at room temperature in chloroform/TFA with a ratio of 3:1 until the formation of a transparent polymer solution. A 10mL syringe filled with the PEICT polymer solution was installed on an electrospinning power supply (Har-100*12, Matsusada Co., Tokyo, Japan) and supplied with a high voltage of 12.5 kV, keeping a distance of 18 cm from the electrospinning tip to the collector. PEICT ENMs were dried in air at room temperature prior to other necessary characterizations.

3.2.3. Characterizations

The in vitro cytocompatibility of PEICT ENMs was analyzed by NIH 3T3 mouse fibroblast cells, DMEM was used with 10% fetal bovine serum (FBS) incubated at 37°C with 5% CO_2. The PEICT ENMs were punched into 3mm disc-shaped webs and poured into 70% ethanol for sterilization, then washed using PBS after 30min of dipping. The sterilized PEICT ENMs were placed in a culture flask. Subsequently, each cell culturing well was seeded with NIH 3T3 cells at (1×10^3) density. The cell culture assessment on PEICT nanofibers was carried for one, three, and seven days, while 10µL WST-1 was added to each flask intermittently after two days. The toxicity, cell proliferation, cell viability, and cell adhesion properties of PEICT ENMs were studied in accordance with the previously reported articles [22,24,25].

The morphology of PEICT ENMs was assessed under (field emission electron microscope (FE-SEM; JEOL JSM 6700 F) by JEOL, Japan with the accelerating voltage of (15kV) and a maximum magnification of 2000, whereas the morphology of PEICT ENMs before and after cell culture was assessed under SEM (JSM-6010LA) by JEOL, Japan with the accelerating voltage of (10kV). A fin coater (JFC-1200) by JEOL, Japan was used for coating PEICT ENMs using Pb-Pt for 120s. The average diameter histogram of PEICT ENMs was calculated using ImageJ software. To investigate the fibroblast cell adhesion and migration on PEICT ENMs, the morphology of fibroblast cells was assessed under scanning electron microscope (SEM) and the images were taken before and after seven days of cell culture. Fibroblast cells, after

seven days of culture, were fixed on the PEICT ENMs with 4% of paraformaldehyde for 4h at 4°C. PEICT ENMs containing the adhered fibroblasts were dehydrated using ethanol and dried in a vacuum prior to taking images [25].

The chemical composition of PEICT ENMs was assessed under Attenuated Total Reflection Fourier-transform infrared spectroscopy (ATR-FTIR) mode using IR Prestige-21, Shimadzu (Kyoto, Japan). Transmittance spectra were assessed in the wavelength range of 670 to 3000 cm^{-1} at room temperature.

The presence of elements available in the PEICT ENMs was checked under XPS supplied from AXIS Ultra (Schimadzu) with a hemispherical sector analyzer (HSA), dual-anode x-ray source Al/Mg, and the detector. A MgKα x-ray source with 1253.6 eV was used at 1.4×10^{-9} torr pressure.

3.3. Results and Discussion

3.3.1. Fibroblast cell culture, adhesion and viability on PEICT ENMs

Fibroblast cells were cultured on PEICT ENMs to check the biocompatibility of these nanofibrous mats [22]. Fig.3.1A shows the microscopic images of the fibroblast cells in the culture flask for one day, three days, and seven days [25]. SEM images were taken after seven days of cell culture on PEICT ENMs, which revealed good cell adhesion as shown in Fig.3.1B. The reason for this may be the smooth morphology of PEICT ENMs and the optimum cellular infiltration into the porous nanofiber mats. The bar graph shown in Fig.3.1C reveals cell viability, which demonstrates that the presence of PEICT ENMs in the culturing environment does not have much negative influence on cell growth, where 85–90% of the healthy cells can survive up to one day (until the first day) of culture. After three days of culture, the number of cells was decreased by 35%, but after seven days, the remaining cells showed very good proliferation and the fibroblast cells had multiplied and reached 70% in parallel to very good cell adhesion. These findings suggest that PEICT ENMs can potentially be considered for fibroblast cell culture application.

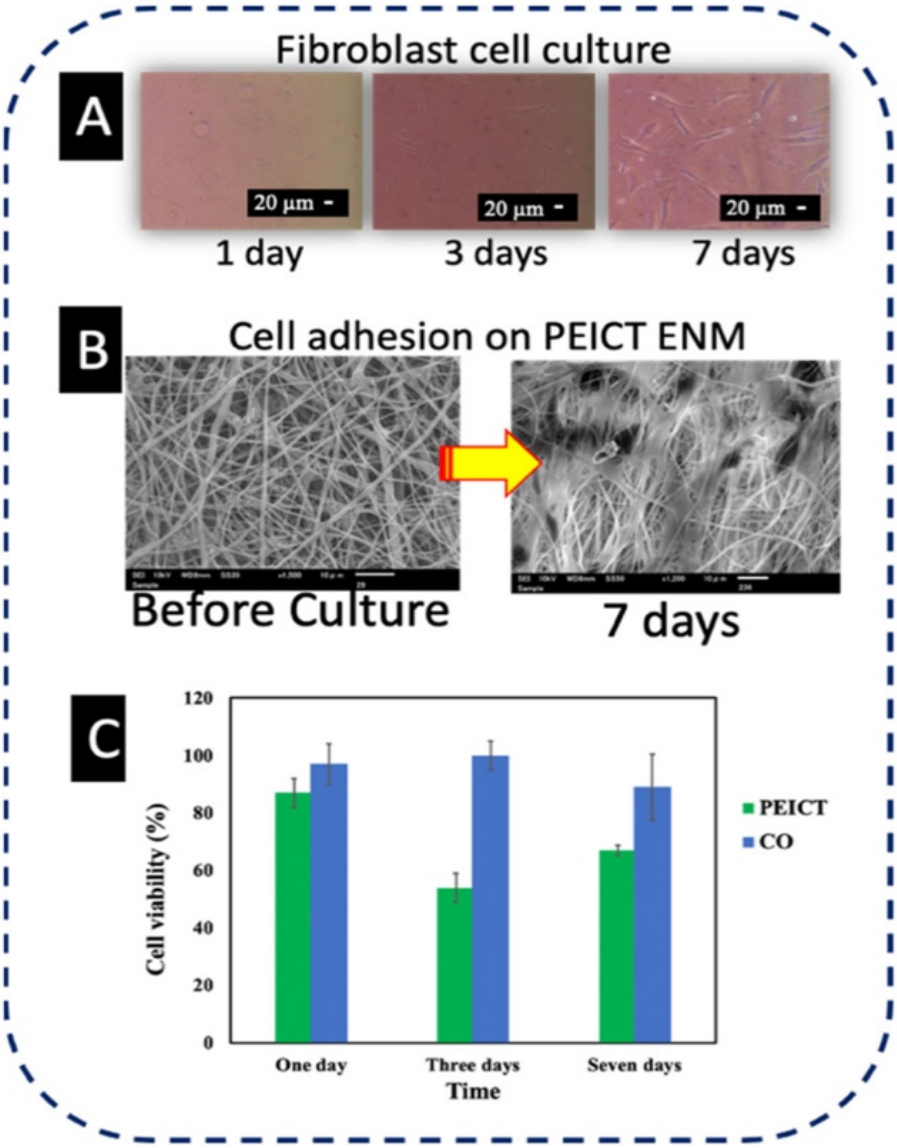

Fig. 3.1. (A) Microscopic images of fibroblast cells in the culture flask. (B) SEM image of cell adhesion of PEICT ENM. (C) Cell viability of PEICT ENMs.

3.3.2. Morphology of PEICT ENMs

To assess the optimized network of nanofibers for the culture and the infiltration of fibroblast cells on the surface of PEICT ENMs, it was necessary to check the morphology and the average fiber diameter of PEICT ENMs. Fig.3.2A shows the bead-free and the smooth morphology of PEICT nanofibers when electrospun with 11% polymer concentration on a rotating cylinder at a speed of 70rpm. Fig.3.2B shows the average diameter distribution graph of PEICT ENMs. The average fiber diameter was found to be 550±60nm, and the average fiber dimeter distributions of PEICT nanofibers ranging from 300nm to 700nm indicates a non-uniform

filtration surface of the PEICT ENM layer, which may be a reason that the infiltration was not 100%.

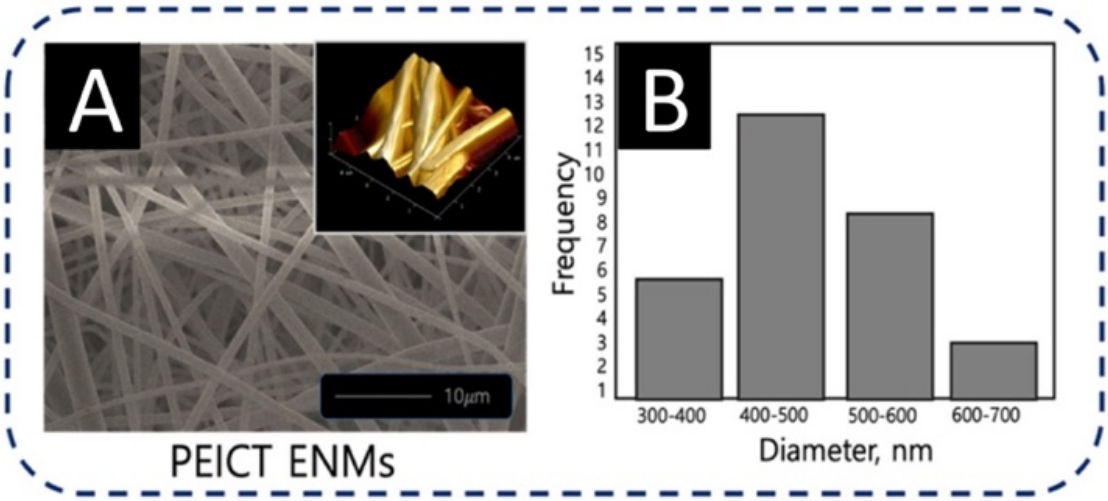

Fig. 3.2. (A) FE-SEM image inset with AFM image, and (B) average diameter histogram of PEICT ENMs.

Compared to the previous reports on PEICT ENMs, this study showed a slightly smaller average fiber diameter size and less diameter distribution as exhibited in the average fiber diameter histogram shown in Fig.3.2B. In addition, the fiber topography on the surface of PEICT ENM, revealed by the inset atomic force microscopic (AFM) image of Fig.3.2A, showed a smaller number of gaps between the nanofibers. Good fibroblast cell adhesion on the PEICT ENM surface was perhaps due to the similar frequency of the nanofibers average diameter, which helped in providing smoothness in parallel to an interconnected nanofiber network to support fibroblast cell infiltration [4,26–29].

3.3.3. FTIR Spectroscopy of PEICT ENMs

Fig.3.3 shows the FTIR spectrum of PEICT ENM. The intensive peak appearing at 1244 cm^{-1} reveals the ethylene glycol present in its chemical structure, which is in agreement with the previous reports [6,8,23]. FTIR spectroscopy further confirms the presence of CH at 2930 cm^{-1} and 726cm^{-1}, C=O at 1715cm^{-1} and CN at 1094cm^{-1}. The abundance of the –CH group on the surface of PEICT ENM may also be the reason for fibroblast cell growth and cell adhesion [29,30].

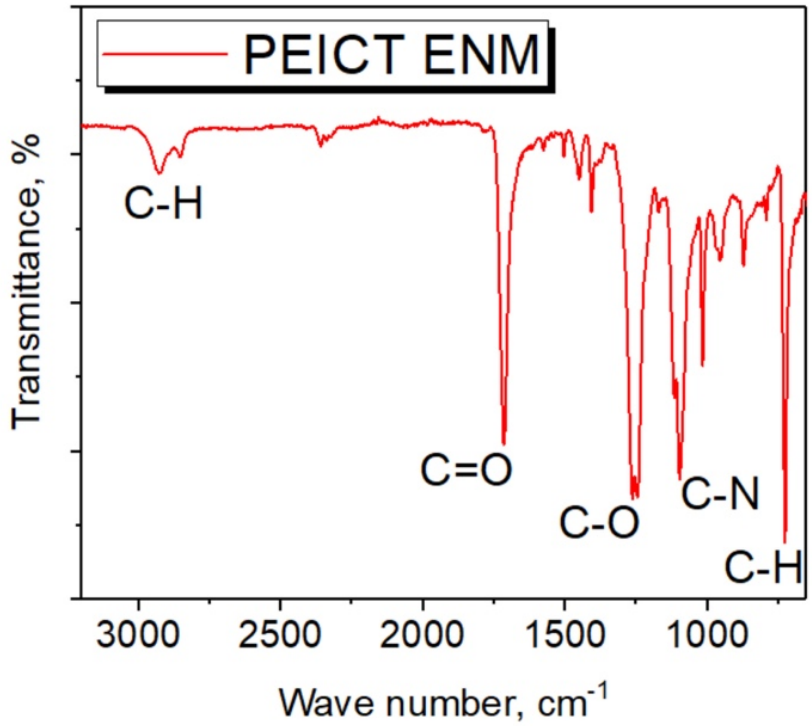

Fig. 3.3. FTIR spectrum of PEICT ENM. *3.4. XPS Spectroscopy of PEICT ENMs*

The main elements present in PEICT ENMs are Isosorbide and ethylene glycol, which were previously reported in published articles and revealed by FTIR spectroscopy [4,6,31]. For a significant chemical composition assessment, we chose XPS spectroscopy to deeply understand the chemical composition of PEICT ENMs.

Fig.3.4 shows the XPS spectra of PEICT ENMs. Fig.3.4A shows the wide XPS spectrum of a PEICT ENM, where two main peaks can be found in the range of Carbon 1s (C1s) and Oxygen 1s (O1s). Therefore, we took XPS spectroscopy of these two intensive regions, C1s ranging from 282eV to 289.5eV and O1s ranging from 528eV and 534eV, while no intensive peak was observed at N1s due to the small amount of the CN group present in the chemical structure of PEICT ENMs. Fig.3.4B demonstrates the XPS spectra in C1s, confirming the –CH group abundance on the surface of the PEICT ENM, and also shows the presence of O=C–O, CN, C–C, C=O, and C–O, demonstrating the chemical composition of PEICT ENM more significantly than FTIR and other previous reports [23,31–34]. The XPS spectra of O1s is given in Fig.3.4C, indicating C=O and C–O present in the chemical composition of PEICT ENM, which validates the results of C1s and FTIR [34,35].

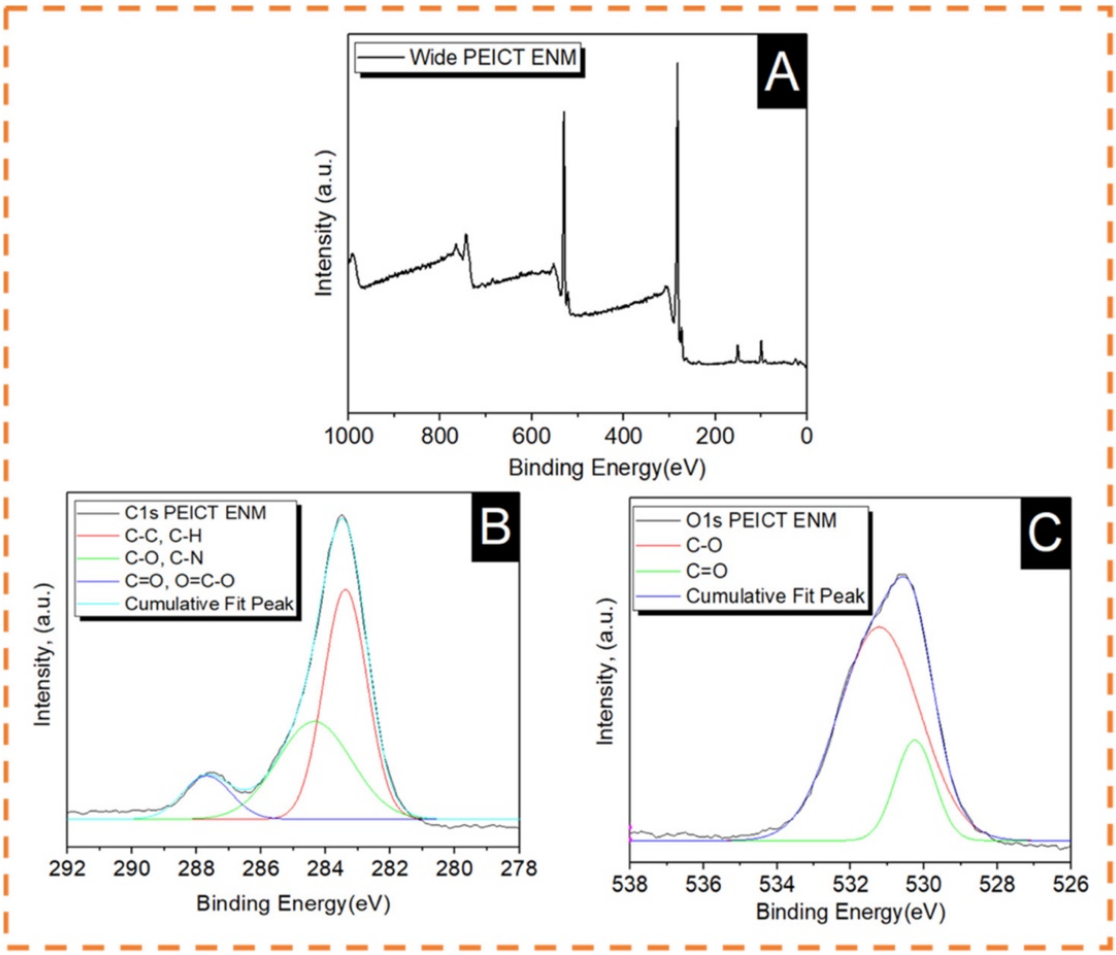

Fig. 3.4. XPS spectra of PEICT ENM. (**A**) Wide spectra. (**B**) Carbon 1s. (**C**) Oxygen 1s.

3.3.4. Wetting Properties of PEICT ENMs

In this report, we cultured fibroblast cells on PEICT nanofibers for the first time, therefore, it was necessary to check the surface wetting properties as one of the important parameters for cell adhesion [27,30]. PEICT ENMs were assessed by the water contact angle (WCA) test [18,36]. Compared to the previous reports on the WCA of PEICT ENMs (114°) [4], the contact angle observed in this study was slightly higher than 120°, where the obvious reason for this was the similar frequency of the nanofibers average diameter, which provided a regular surface with finer fibers that led the water droplet being stable for a certain time prior to starting adsorption on PEICT ENMs. According to Fig.3.5, the water droplet took about 270s to reach the angle 0° from 120°, which is in the range of hydrophobic surfaces. Even though the surface of PEICT ENM is hydrophobic [37], the cell infiltration observed was very good because of the interconnected nanofiber network with a smooth morphology, which also played an

important role in cell adhesion. Additionally, the WCA test suggested that five minutes were enough as a resting period for fibroblast initial cell adherence on PEICT ENMs.

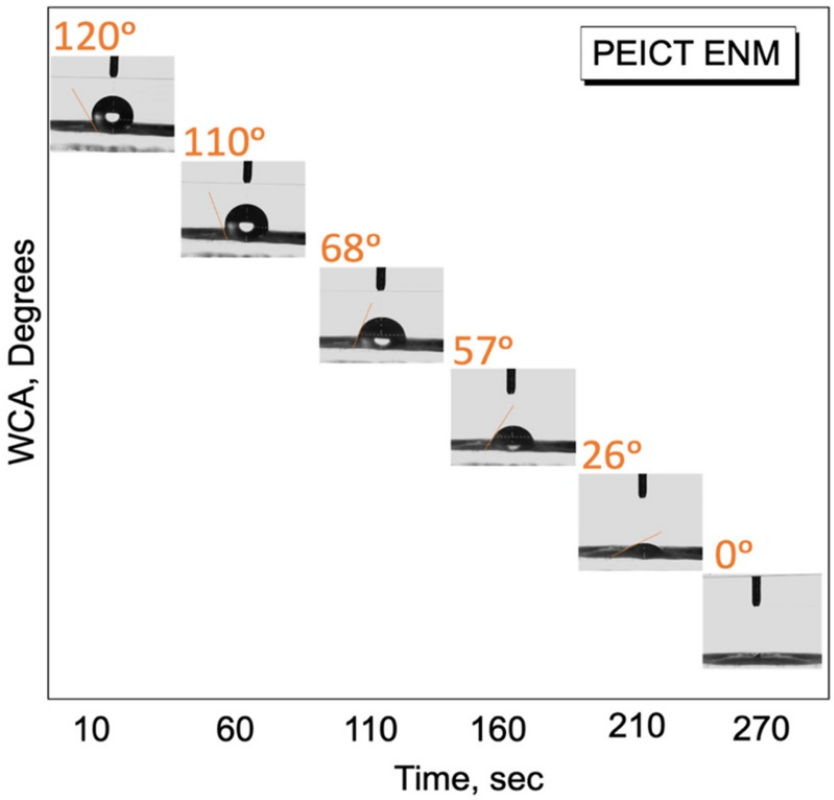

Fig. 3.5. Water contact angle test of PEICT ENMs.

3.4. Conclusion

PEICT ENMs were successfully electrospun at 11% w/w polymer concentration, the electrospun PEICT nanofibers showed bead-free and smooth morphology with an average diameter of 550±60 nm, having less diameter distributions compared to previous reports on electropun PEICT nanofibers. SEM images showed a good cell viability (70%) and cell adhesion properties on the surface of PEICT ENMs after seven days of cell culture. FTIR and XPS spectroscopies confirmed the chemical structure of PEICT ENMs and the bulk presence of the –CH group on its surface, which was one of the reasons for the good cell adhesion. The results manifested a dependency of the cell infiltration on the fiber network and the average diameter of PEICT ENMs. Ultimately, less gaps on the surface of PEICT ENMs may be a reason for cell infiltration. The WCA test revealed the hydrophobic behavior of the mats with an average WCA of 120°, which demonstrated the optimum duration of 5min for the initial resting of cells for their culture prior to starting their culture on PEICT ENMs. Therefore, the results confirmed the potential of PEICT ENMs for fibroblast cell culture application.

3.5. References

1. Kasmi, N.; Pinel, C.; Perez, D.D.S.; Dieden, R.; Habibi, Y. Synthesis and characterization of fully biobased polyesters with tunable branched architectures. *Polym. Chem.* 2021, *12*, 991–1001.
2. Bansal, K.K.; Rosenholm, J.M. Synthetic polymers from renewable feedstocks: An alternative to fossil-based materials in biomedical applications. *Ther. Deliv.* 2020, *11*, 297–300.
3. Prabakaran, R.; Marie, J.M.; Xavier, A.J.M. Biobased Unsaturated Polyesters Containing Castor Oil-Derived Ricinoleic Acid and Itaconic Acid: Synthesis, In Vitro Antibacterial, and Cytocompatibility Studies. *ACS Appl. Bio Mater.* 2020, *3*, 5708–5721.
4. El-Ghazali, S.; Khatri, M.; Hussain, N.; Khatri, Z.; Yamamoto, T.; Kim, S.H.; Kobayashi, S.; Kim, I.S. Characterization and biocom- patibility evaluation of artificial blood vessels prepared from pristine poly (Ethylene-glycol-co-1, 4-cyclohexane dimethylene- co-isosorbide terephthalate), poly (1, 4 cyclohexane di-methylene-co-isosorbide terephthalate) nanofibers and their blended composition. *Mater. Today Commun.* 2021, *26*, 102113.
5. Das, S.S.; Bharadwaj, P.; Bilal, M.; Barani, M.; Rahdar, A.; Taboada, P.; Bungao, S.; Kyzas, G.Z. Stimuli-Responsive Polymeric Nanocarriers for Drug Delivery, Imaging, and Theragnosis. *Polymers* 2020, *12*, 1397.
6. Khan, M.Q.; Lee, H.; Khatri, Z.; Kharaghani, D.; Khatri, M.; Ishikawa, T.; Im, S.S.; Kim, I.S. Fabrication and characterization of nanofibers of honey/poly (1, 4-cyclohexane dimethylene isosorbide trephthalate) by electrospinning. *Mater. Sci. Eng. C* 2017, *81*, 247–251.
7. Park, S.; Thanakkasaranee, S.; Shin, H.; Ahn, K.; Sadeghi, K.; Lee, Y.; Tak, G.; Seo, J. Preparation and characterization of heat-resistant PET/bio-based polyester blends for hot-filled bottles. *Polym. Test.* 2020, *91*, 106823.
8. Lee, H.; Koo, J.M.; Sohn, D.; Kim, I.S.; Im, S.S. High thermal stability and high tensile strength terpolyester nanofibers containing biobased monomer: Fabrication and characterization. *RSC Adv.* 2016, *6*, 40383–40388.
9. Legrand, S.; Jacquel, N.; Amedro, H.; Saint-Loup, R.; Pascault, J.P.; Rousseau, A.; Fenouillot, F. Synthesis and properties of poly (1, 4-cyclohexanedimethylene-co-isosorbide terephthalate), a biobased copolyester with high performances. *Eur. Polym. J.* 2019, *115*, 22–29.
10. Bui, H.T.; Chung, O.H.; Cruz, J.D.; Park, J.S. Fabrication and characterization of electrospun curcumin-loaded polycaprolactone- polyethylene glycol nanofibers for enhanced wound healing. *Macromol. Res.* 2014, *22*, 1288–1296.
11. Lanzalaco, S.; Del Valle, L.J.; Turon, P.; Weis, C.; Estrany, F.; Alemán, C.; Armelin, E. Polypropylene mesh for hernia repair with controllable cell adhesion/de-adhesion properties. *J. Mater. Chem. B* 2020, *8*, 1049–1059.
12. Cavalcanti-Adam, E.A. Building nanobridges for cell adhesion. *Nat. Mater.* 2019, *18*, 1272–1273.
13. Khatri, Z.; Jatoi, A.W.; Ahmed, F.; Kim, I.S. Cell adhesion behavior of poly (ε-caprolactone)/poly (L-lactic acid) nanofibers scaffold. *Mater. Lett.* 2016, *171*, 178–181.
14. Khatri, M.; Ahmed, F.; Ali, S.; Mehdi, M.; Ullah, S.; Duy-Nam, P.; Khatri, Z.; Kim, I.S. Photosensitive nanofibers for data recording and erasing. *J. Text. Inst.* 2021, *112*, 429–436.

15. Udomluck, N.; Lee, H.; Hong, S.; Lee, S.H.; Park, H. Surface functionalization of dual growth factor on hydroxyapatite-coated nanofibers for bone tissue engineering. *Appl. Surf. Sci.* 2020, *520*, 146311.
16. Khatri, M.; Ahmed, F.; Shaikh, I.; Phan, D.N.; Khan, Q.; Khatri, Z.; Lee, H.; Kim, I.S. Dyeing and characterization of regenerated cellulose nanofibers with vat dyes. *Carbohydr. Polym.* 2017, *174*, 443–449.
17. Khatri, M.; Ahmed, F.; Jatoi, A.W.; Mahar, R.B.; Khatri, Z.; Kim, I.S. Ultrasonic dyeing of cellulose nanofibers. *Ultrason. Sonochem.* 2016, *31*, 350–354.
18. Khatri, M.; Khatri, Z.; El-Ghazali, S.; Hussain, N.; Qureshi, U.A.; Kobayashi, S.; Ahmed, F.; Kim, I.S. Zein nanofibers via deep eutectic solvent electrospinning: Tunable morphology with super hydrophilic properties. *Sci. Rep.* 2020, *10*, 1–11.
19. Cheng, P.; Wang, X.; Liu, Y.; Kong, C.; Liu, N.; Wan, Y.; Guo, Q.; Liu, K.; Lu, Z.; Li, M.; et al. Ag nanoparticles decorated PVA-co-PE nanofiber-based membrane with antifouling surface for highly efficient inactivation and interception of bacteria. *Appl. Surf. Sci.* 2020, *506*, 144664.
20. Fahimirad, S.; Fahimirad, Z.; Sillanpää, M. Efficient removal of water bacteria and viruses using electrospun nanofibers. *Sci. Total Environ.* 2020, *751*, 141673.
21. Phan, D.N.; Khan, M.Q.; Nguyen, N.T.; Phan, T.T.; Ullah, A.; Khatri, M.; Kien, N.N.; Kim, I.S. A review on the fabrication of several carbohydrate polymers into nanofibrous structures using electrospinning for removal of metal ions and dyes. *Carbohydr. Polym.* 2020, *252*, 117175.
22. Ullah, A.; Saito, Y.; Ullah, S.; Haider, M.K.; Nawaz, H.; Duy-Nam, P.; Kharaghani, D.; Kim, I.S. Bioactive Sambong oil-loaded electrospun cellulose acetate nanofibers: Preparation, characterization, and in-vitro biocompatibility. *Int. J. Biol. Macromol.* 2021, *166*, 1009–1021.
23. Phan, D.N.; Lee, H.; Choi, D.; Kang, C.Y.; Im, S.S.; Kim, I.S. Fabrication of Two Polyester Nanofiber Types Containing the Biobased Monomer Isosorbide: Poly (Ethylene Glycol 1,4-Cyclohexane Dimethylene Isosorbide Terephthalate) and Poly (1,4-Cyclohexane Dimethylene Isosorbide Terephthalate). *Nanomaterials* 2018, *8*, 56.
24. Kharaghani, D.; Gitigard, P.; Ohtani, H.; Kim, K.O.; Ullah, S.; Saito, Y.; Kim, I.S. Design and characterization of dual drug delivery based on in-situ assembled PVA/PAN core-shell nanofibers for wound dressing application. *Sci. Rep.* 2019, *9*, 1–11.
25. Kharaghani, D.; Jo, Y.K.; Khan, M.Q.; Jeong, Y.; Cha, H.J.; Kim, I.S. Electrospun antibacterial polyacrylonitrile nanofiber membranes functionalized with silver nanoparticles by a facile wetting method. *Eur. Polym. J.* 2018, *108*, 69–75.
26. Mirticˇ, J.; Balažic, H.; Zupancˇicˇ, Š.; Kristl, J. Effect of Solution Composition Variables on Electrospun Alginate Nanofibers: Response Surface Analysis. *Polymers* 2019, *11*, 692.
27. Han, D.G.; Ahn, C.B.; Lee, J.H.; Hwang, Y.; Kim, J.H.; Park, K.Y.; Lee, J.W.; Son, K.H. Optimization of Electrospun Poly(caprolactone) Fiber Diameter for Vascular Scaffolds to Maximize Smooth Muscle Cell Infiltration and Phenotype Modulation. *Polymers* 2019, *11*, 643.
28. Habib, S.; Zavahir, S.; Abusrafa, A.E.; Abdulkareem, A.; Sobolcˇiak, P.; Lehocky, M.; Vesela, D.; Humpolícˇek, P.; Popelka, A. Slippery Liquid-Infused Porous Polymeric Surfaces Based on Natural Oil with Antimicrobial Effect. *Polymers* 2021, *13*, 206.
29. Dong, X.; Yuan, X.; Wang, L.; Liu, J.; Midgley, A.C.; Wang, Z.; Wang, K.; Liu, J.; Zhu, M.; Kong, D. Construction of a bilayered vascular graft with smooth internal surface for improved hemocompatibility and endothelial cell monolayer formation. *Biomaterials* 2018, *181*, 1–14.

30. Arima, Y.; Iwata, H. Effect of wettability and surface functional groups on protein adsorption and cell adhesion using well-defined mixed self-assembled monolayers. *Biomaterials* 2017, *28*, 3074–3082.
31. Yoon, W.J.; Hwang, S.Y.; Koo, J.M.; Lee, Y.J.; Lee, S.U.; Im, S.S. Synthesis and Characteristics of a Biobased High-Tg Terpolyester of Isosorbide, Ethylene Glycol, and 1,4-Cyclohexane Dimethanol: Effect of Ethylene Glycol as a Chain Linker on Polymerization. *Macromolecules* 2013, *46*, 7219–7231.
32. Yu, Y.; Jiang, X.; Fang, Y.; Chen, J.; Kang, J.; Cao, Y.; Xiang, M. Investigation on the Effect of Hyperbranched Polyester Grafted Graphene Oxide on the Crystallization Behaviors of β-Nucleated Isotactic Polypropylene. *Polymers* 2019, *11*, 1988.
33. Narayanan, G.; Shen, J.; Boy, R.; Gupta, B.S.; Tonelli, A.E. Aliphatic Polyester Nanofibers Functionalized with Cyclodextrins and Cyclodextrin-Guest Inclusion Complexes. *Polymers* 2018, *10*, 428.
34. Zhang, W.; Zheng, C.; Zhang, Y.; Guo, W. Preparation and Characterization of Flame-Retarded Poly(butylene terephtha- late)/Poly(ethylene terephthalate) Blends: Effect of Content and Type of Flame Retardant. *Polymers* 2019, *11*, 1784.
35. Mehdi, M.; Mahar, F.K.; Qureshi, U.A.; Khatri, M.; Khatri, Z.; Ahmed, F.; Kim, I.S. Preparation of colored recycled polyethylene terephthalate nanofibers from waste bottles: Physicochemical studies. *Adv. Polym. Technol.* 2018, *37*, 2820–2827.
36. Khatri, M.; Hussain, N.; El-Ghazali, S.; Yamamoto, T.; Kobayashi, S.; Khatri, Z.; Kim, I.S. Ultrasonic-assisted dyeing of silk fibroin nanofibers: An energy-efficient coloration at room temperature. *Appl. Nanosci.* 2020, *10*, 917–930.
37. Chen, C.Y.; Huang, S.Y.; Wan, H.Y.; Chen, Y.T.; Yu, S.K.; Wu, H.C.; Yang, T.I. Electrospun Hydrophobic Polyaniline/Silk Fibroin Electrochromic Nanofibers with Low Electrical Resistance. *Polymers* 2020, *12*, 2102.

CHAPTER 4 Preparation of a Cage-Type Polyglycolic Acid/Collagen Nanofiber Blend with Improved Surface Wettability and Handling Properties for Potential Biomedical Applications

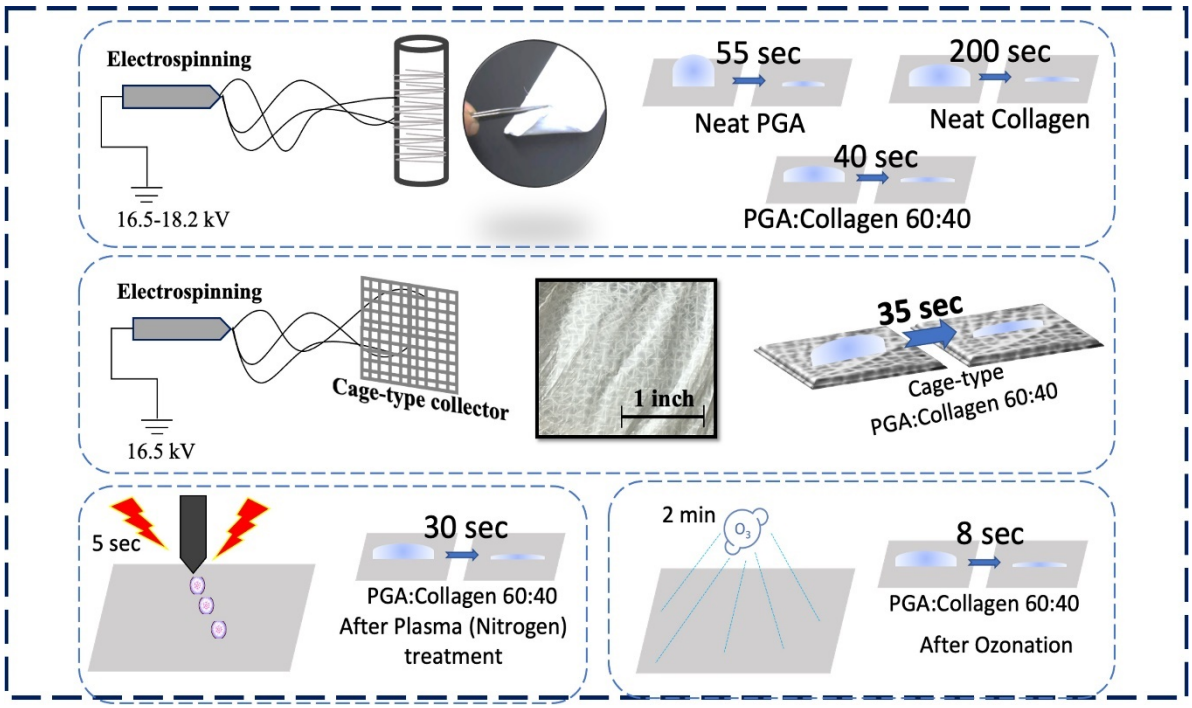

4.1. Introduction

Recently, many scientists have been exploring the biomedical properties of different polymeric materials, and the preparation of such materials with multiple desired characteristics has remained a challenging task [1–4]. In the last few years, there has been a growing interest in Polyglycolic acid (PGA), collagen and their blended compositions incorporated with different functional guest materials for various targeted applications [5–7]. Only few reports could be found regarding electrospun PGA, collagen nanostructures and their blends incorporated with external functional guest materials to improve surface properties viz. wettability and morphology, and this remains a big research gap [8–11].

PGA-based copolymers have been considered as green polymers [1,6] with good biodegradability [6] and mechanical properties [12], high heat distortion temperature [13], good biocompatibility [14], cell viability and very low solubility in organic solvents [15,16]. In the form of nanofibers, PGA-based copolymers have exclusive scaffolding properties for tissue regeneration, comparatively faster than polyesters, polycaprolactone (PCL) and polybutylene adipate-co-terephthalate (PBAT), which reveals a higher level of suitability of PGA for biomedical applications [6,17]. In parallel, collagen has also been utilized for several biomedical applications because of its biological characteristics, such as biodegradability,

biocompatibility, low immunogenicity, easy processing and hydrophilicity [7]. It is well known that mammals contain an abundant amount of collagen in their structural protein, which has been utilized in various forms, such as membrane, hydrogel, powder, sponge and fibers [9–11]. Functionally, collagens are complex and structurally diverse. The literature confirms that collagen can perform well even when composited in the shape of fibers and utilized for potential biomedical applications in parallel to good physicochemical and mechanical properties [15,16]. Furthermore, collagen constitutes a fundamental part of the skin, tendons, sclera, ligaments, cartilage, cornea and bones [9,15]. The bulk presence of collagen in animals shows its biocompatibility, and materials based on collagen may be utilized to assist surgical operations [9–15]. Thus, both PGA and collagen are considered as biomaterials and have been utilized for applications where self-supramolecular assembly, an extracellular matrix structure (ECM) interface and good bio-induction are required. However, these biomaterials may lose their originality when blended with external substrates to impart required characteristics such as tunable wettability. To prevent the latter issue, optimization using external surface treatments viz. plasma/ozonation or the incorporation of functional materials is needed [15–17].

PGA/collagen nanofiber-based scaffolds have very good cell adhesion and cell growth properties but are not sufficient for other practical applications, such as bleeding control during surgeries [18–25], material flexibility and easy handling during surgeries [19–22]. These critical issues during surgeries can be addressed by modifying the surface and handling properties [22–30]. Therefore, a blended composition is necessary to impart suitable surface properties onto the optimized nanofibers in order to achieve an ease in handling and the ability to control severe bleeding during surgical operations [24,25,27]. Changes in the surface properties of electrospun biomaterials, such as texture, wettability and present functional groups [3,26], can be altered either via surface treatments (i.e. plasma/ozonation) or by incorporating functional guest molecules which may introduce required chemical groups on the surface [31–36].

Nanofibers possess a high surface area, a very fine fiber diameter and have been utilized for multipurpose applications, including tissue engineering [37–41], smart apparel and environmental applications due to the ease of their production [42–48]. Their high breathability, light weight, biocompatibility and three-dimensional morphology make them a porous matrix which resembles the native ECM [38–40]. Nanofiber-based composites, due to their considerable ease of handling and their optimized surface properties, can be potentially utilized for assisting biomedical surgical operations [49,50].

Ultimately, the optimal wettability of polymeric materials has been considered as an important parameter for cell culture and cell adhesion [51–57]. Therefore, a bio-based cage-type nanofiber blend PGA/collagen was prepared using a cage-type collector during electrospinning, and the effect of ozonation and plasma treatments was assessed. As PGA and Collagen are already reported as biocompatible polymers, instead of performing cell culture on PGA and Collagen based nanofibers, we have limited this study to the achievement of enhanced wettability with different surface textures and improved handling properties. Additionally, two concentrations of poly (α, β-malic acid) (SuPMA) were incorporated into the cage-type blend [58], and the wettability was checked using the WCA test, supported by Raman and FTIR spectroscopy.

4.2. Experimental Section

4.2.1. Materials

PGA, lyophilized type I collagen (derived from porcine tissue) and chemical grade 1,1,1,3,3,3 hexafluoro-2-propanol (HFIP) were purchased from Sigma-Aldrich, Ltd., Osaka, Japan. SuPMA was synthesized as per the method used in a previous study [58].

4.2.2. Preparation of PGA and Collagen and Cage-Type Nanofiber Blend via Electrospinning

Both PGA and collagen polymer solutions were separately prepared with 10% (w/v) polymer concentration in HFIP. PGA and collagen were dissolved at 70℃ and 4℃ for 80h and 24h, respectively. Collagen and PGA were blended at different ratios (60:40, 50:50 and 40:60 (v/v)). The blends of PGA/collagen were poured into a 10mL syringe affixed with a 22-gauge stainless needle, and the feed rate of the syringe pump (780100J, KD Science, Holliston, MA, USA) was set at 0.4–0.7mL/h. A high-voltage (16.5–18.2) kV was supplied to the needle using an HSP-30K-2 (Nippon Stabilizer Industry Co. Ltd., Osaka, Japan), keeping the bead-free nanofibers production in consideration while electrospinning for 4.5h at room temperature with a humidity maintained at 30±6% by the perfusion of nitrogen. A cage-type metallic collector with pore size 2×2mm2 and a plain metallic plate were used for the collection of nanofibers during electrospinning. All blended compositions of nanofiber mats were peeled and air dried before further assessment [32]. Fig.4.1 shows the electrospinning process and resultant of the cage-type nanofibers along with an inset SEM image, revealing the smooth and bead-free morphology of nanofiber mats.

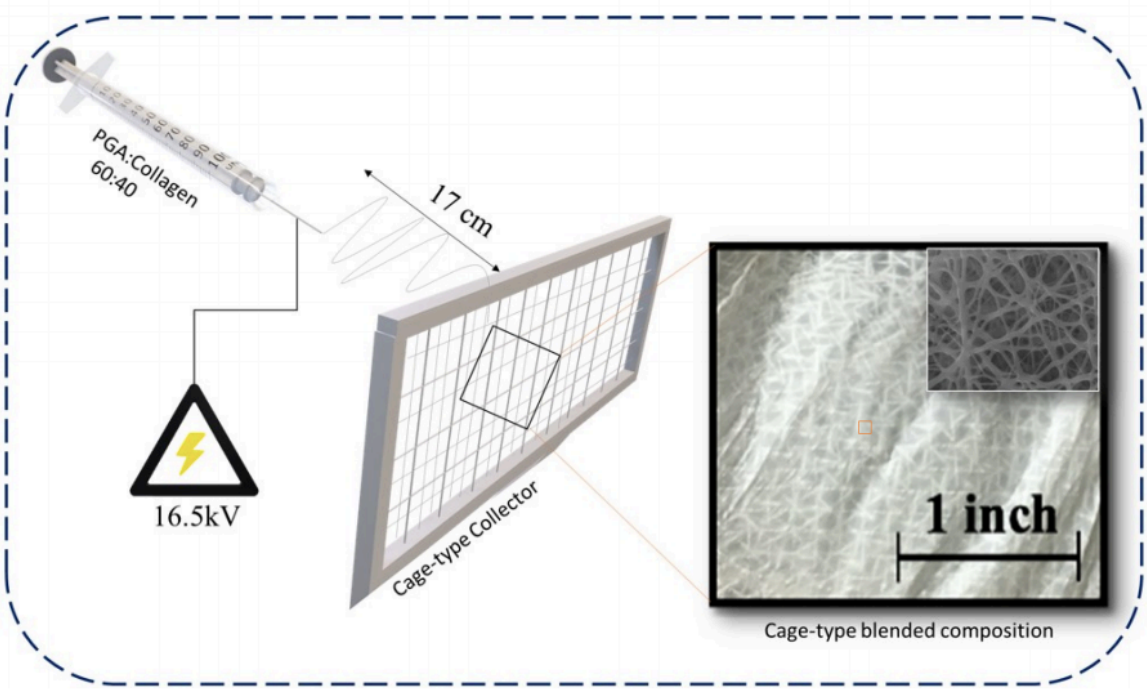

Fig.4.1. Preparation of cage-type PGA/collagen 60:40 nanofiber blend.

4.3. Characterization

4.3.1. Scanning Electron Microscopy (SEM)

Neat PGA, neat collagen and all treated (using plasma and ozonation) and untreated blended nanofiber composites were examined under SEM (JEOL-5600LV, Japan) at an accelerating voltage of 20kV. A JEOL-JED2200 (Japan) was used to carry out EDS and the samples were coated with tungsten and platinum for the morphological observations using Elionics-E101. The average diameter histogram of all nanofiber samples was analyzed using SEM JEOL-5600LV-based software.

4.3.2. Fourier Transform Infrared (FTIR) Spectroscopy

All nanofiber samples were assessed using IR Prestige-21, Shimadzu (Kyoto, Japan) in ATR-FTIR mode at an adsorption wavelength between 1000cm^{-1} and 4000cm^{-1} at 25˚C.

4.3.3. Water Contact Angle (WCA) Test

The WCA was measured using the static angle by a drop testing method, keeping the drop size at 1µL. The average taken from 15 measurements was considered from 1 to 300s. FACE model CA-VP, Kyowa interface science, Japan was used to check the WCA of neat PGA, collagen, their blended compositions, plasma-treated PGA, collagen, their blended compositions, ozone-

treated PGA, collagen, their blended compositions and the neat cage-type blend with and without the incorporation of SuPMA.

4.3.4. Raman Spectroscopy

The Raman spectra of the cage-type PGA/collagen was checked using Raman Touch VIS-NIR, Nano photon, and the results were recorded at room temperature in the range between 800cm^{-1} and 4000cm^{-1} .

4.4. Results and Discussion

4.4.1. Morphology of PGA, Collagen, and their Blend Nanofibers

Electrospinning of neat PGA with a concentration of 10% showed a bead-free morphology with the random deposition of fine nanofibers with an average diameter of 180±30nm, as shown in Fig.4.2A. Neat collagen showed thick nanofibers with an average diameter of 500±40nm, as revealed in Fig.4.2B. The PGA/collagen nanofibers with an optimized ratio of 60:40 showed a bead-free, smoother morphology and regular deposition compared to neat PGA and neat collagen nanofibers, as revealed in Fig.4.2C. An average diameter distribution of 300±20nm was observed for the blended composition, which is between the average nanofiber diameter of neat PGA and neat collagen. In addition, SEM-EDS confirmed the presence of both PGA and collagen in the resultant blend, and an abundancy of oxygen from PGA $(C_2H_2O_2)_n$ and nitrogen from collagen $(C_{57}H_{91}N_{19}O_{16})$ can clearly be seen in the PGA/collagen 60:40 blend, as per the inset EDS graphs given in Fig.4.2A–C, respectively.

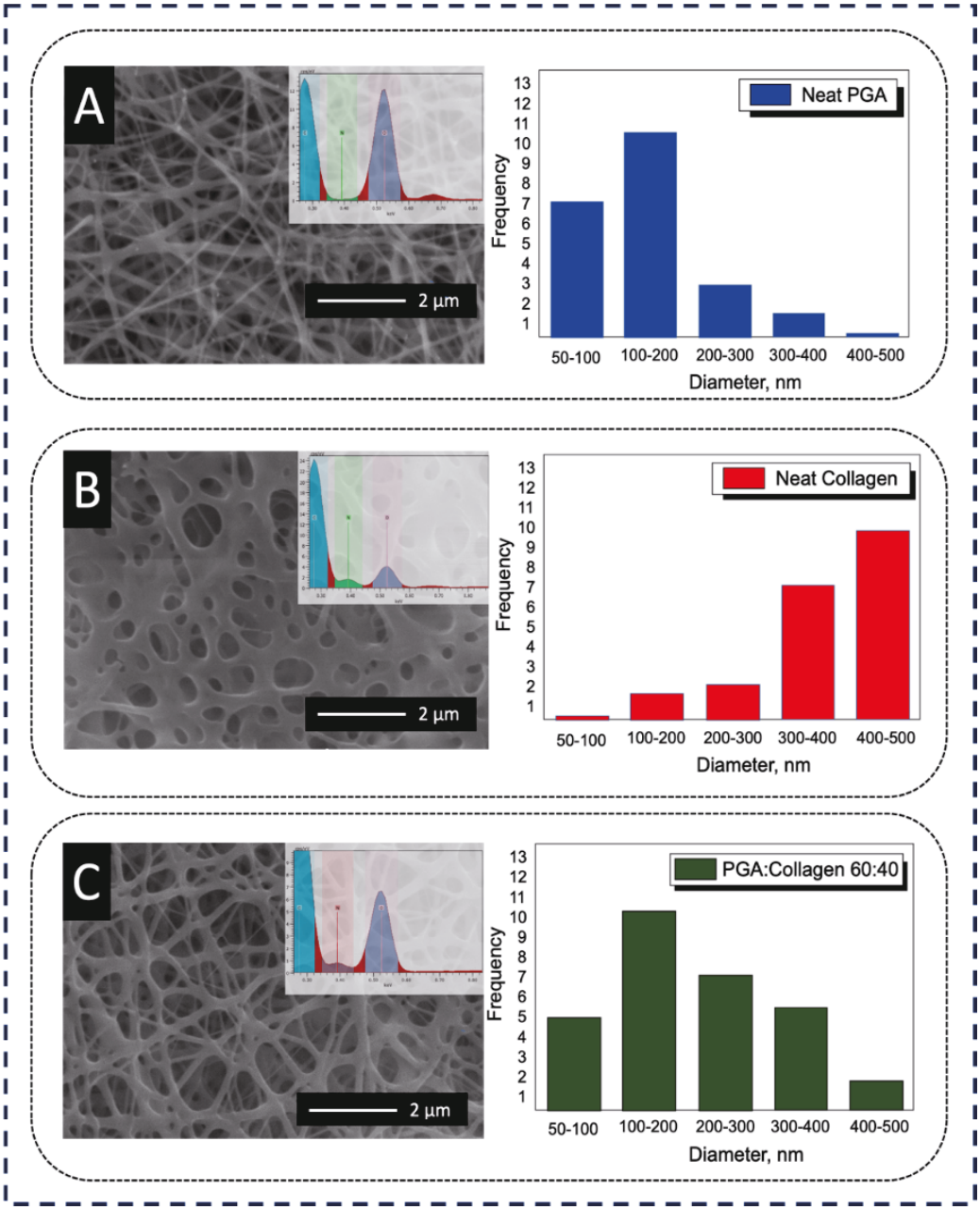

Fig. 4.2. SEM images, EDS and diameter distributions histogram of (A) neat PGA, (B) neat collagen, (C) PGA/collagen (60:40).

4.4.2. Effect of Ozonation and Plasma treatment on the morphology of PGA/Collagen Blends

The choice of PGA/collagen 60:40 as the optimized blend was based on the comparison of the morphology of three ratios of PGA/collagen blends after ozonation (O3) and plasma (nitrogen) treatment. Ozonation and plasma treatments impart respective functional groups on the surface of suitable substrate. To treat surfaces, a constant time slot was fixed individually for ozonation (2min) and plasma treatment (5s) on each blended composition of PGA and collagen. Fig.4.3A shows thick nanofibers in PGA/collagen 40:60; during ozonation, the fibers were degraded at

a certain level, and after plasma treatment, the fibers were semi-stable with a slight degradation. Comparatively, finer fibers in PGA/collagen 50:50 were observed, as shown in Fig.4.3B; this blend was slightly less degraded than the PGA/collagen 40:60. A root-shaped morphology was observed due to the breakage by plasma treatment pressure on the surface of PGA/collagen 50:50 nanofibers, and the nanofibers became comparatively thinner than the untreated PGA/collagen 50:50. Fig.4.3C reveals a slight degradation of PGA/collagen 60:40 on ozonation with fine and stable nanofiber morphology, whereas plasma treatment did not show any negative influence in the blended composition of PGA/collagen 60:40. In parallel to the smooth, regular and stable morphology of the PGA/collagen 60:40 blend, very good handling properties were observed. Thus, PGA/collagen 60:40 can be considered for its optimization and utilization in surgical operations.

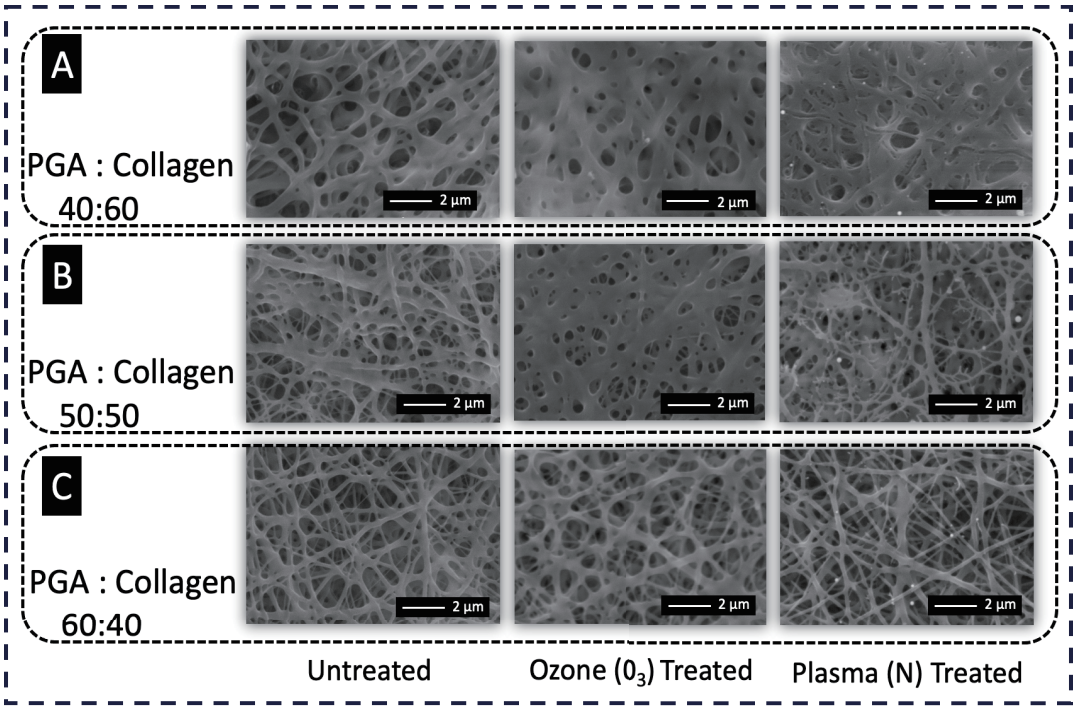

Fig. 4.3. SEM images of untreated, ozone (O_3)-treated, and plasma (N)-treated (A) PGA/collagen nanofibers with ratio 40:60, (B) PGA/collagen nanofibers with ratio 50:50 and (C) PGA/collagen nanofibers with ratio 60:40

4.4.3. Chemical Properties of PGA, Collagen, and their blend nanofibers

Neat PGA, neat collagen and three different blends were assessed using FTIR spectroscopy, as shown in Fig.4.4. Neat PGA shows two big stretching peaks of C–O and C=O at 1148cm^{-1} and 1752cm^{-1}, respectively, and one small peak at 1081cm^{-1}, confirming the bulk presence of C–O groups. The FTIR spectrum of PGA shows a bending peak at 1417cm^{-1}, revealing OH

presence within the chemical structure of neat PGA nanofibers, whereas it does not show any peak of the OH group in the range near 3300cm^{-1}.

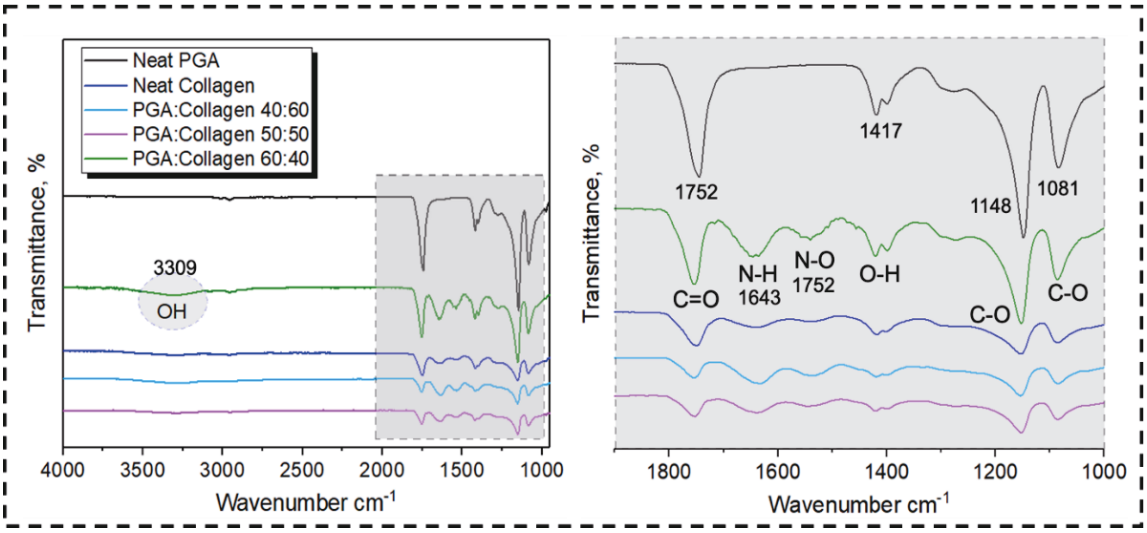

Fig. 4.4. FTIR spectrum of neat PGA, neat collagen and their blended compositions.

On the other hand, neat collagen showed a raising peak at 3309cm^{-1}, confirming the presence of an OH group on its surface, and a small bend at 1417cm^{-1} represents OH groups within the chemical composition of collagen nanofibers. The FTIR spectrum further shows NH at 1643cm^{-1} and also demonstrates the presence of NO and OH at small peaks between 1400cm^{-1} and 1600cm^{-1}. Similar to neat PGA, neat collagen also has stretching peaks at 1081cm^{-1}, and at 1148cm^{-1} revealing the presence of C-O in its chemical structure. Neat PGA has more intensive peaks due to the bulk presence of chemical groups on its surface. therefore, PGA/collagen 40:60 did not show any intensive peaks at any point of the FTIR spectrum; even in the blends of PGA/collagen 50:50, some small peaks slightly appeared, confirming the blending of PGA and collagen, while in the case of PGA/collagen 60:40, the peaks became intensive with clear stretching and bending, resulting in more visible OH groups on the surface of the blended composition compared to neat collagen, as per the given FTIR results. The FTIR spectra of blended PGA/collagen 60:40 shows a higher number of NH, C-O and N-O groups compared to the groups present in other PGA/collagen blends. Bulk functional groups on the blend surface have a direct impact on the wettability of polymeric fibers, which, according to the literature, may offer very good cell culture and adhesion properties compared to those with low surface wettability [52,54,55].

4.4.4. Effect on the wettability of neat PGA, Collagen and their blends nanofibers

4.4.4.1. Ozonation and Plasma Treatment Effect on the Wettability of Nanofibers

The effects of ozonation and plasma treatments on the wettability of neat and blended compositions of PGA and collagen nanofibers were determined using WCA test.

FTIR results revealed the bulk presence of OH and NH groups on the surface of PGA/collagen with the ratio of 60:40, which was an indication of some change in the wettability on its surface. Fig.4.5A shows the water contact angle (WCA) test of PGA/collagen nanofibers with the blend ratios of 40:60, 50:50 and 60:40 and with water contact angles between 20° and 25°. The PGA/collagen 40:60 took 170s to completely absorb the droplet on its surface suggesting its hydrophobic behavior. Decreasing the collagen polymer concentration to 50% into the blended composition resulted in decreased hydrophobicity, which took 135s to completely absorb the droplet as compared to the blend containing 60% of collagen. FTIR spectroscopy did not show any significant difference in the chemical structure of PGA/collagen with ratios 40:60 and 50:50 due to the small difference in the composition blends, only the change in wettability showed the difference in blended composition which was due to more PGA content. WCA of PGA/collagen 60:40 demonstrated only 40s to completely absorb the water droplet on its surface while the contact angle was 20° , which is considered as hydrophilic, the reason to this was the presence of more NH and OH groups on its surface as confirmed by FTIR spectroscopy. WCA test revealed that the simple blending process of polymers (PGA and collagen) at room temperature in the presence of solvent (HFIP) can impart more functional groups on the surface of resultant PGA/collagen 60:40 nanofibers. Fig.4.5B shows the WCA of untreated, ozone treated and plasma treated PGA nanofibers. WCA of neat PGA nanofibers did not show very good hydrophilic properties with droplet absorption to 0° from 120° in 55s, which is comparatively less hydrophilic than the optimized blend of PGA/collagen with ratio 60:40. PGA on 2min of ozonation, and 5s of plasma treatment increased the wettability to super hydrophilic range with reduced droplet adsorption time to 1s, whereas the initial contact angle was <10°. In Fig.4.5C, collagen also showed increased wettability with decreased time for complete droplet adsorption but still remained in the category of hydrophobic revealing 200s, 110s and 180s for untreated, ozone treated and plasma treated collagen nanofibers having contact angles 36°, 23° and 23° respectively. The optimized blended composition PGA/collagen with ratio 60:40 was also treated using ozone and plasma, and assessed under WCA test as shown in Fig.4.5D. Neat PGA/collagen 60:40 took 40s, ozone treated blend took

8s, plasma treated sample took 30s for complete droplet absorption on their surfaces, whereas, the contact angles were observed as 20°, 50° and 21° respectively.

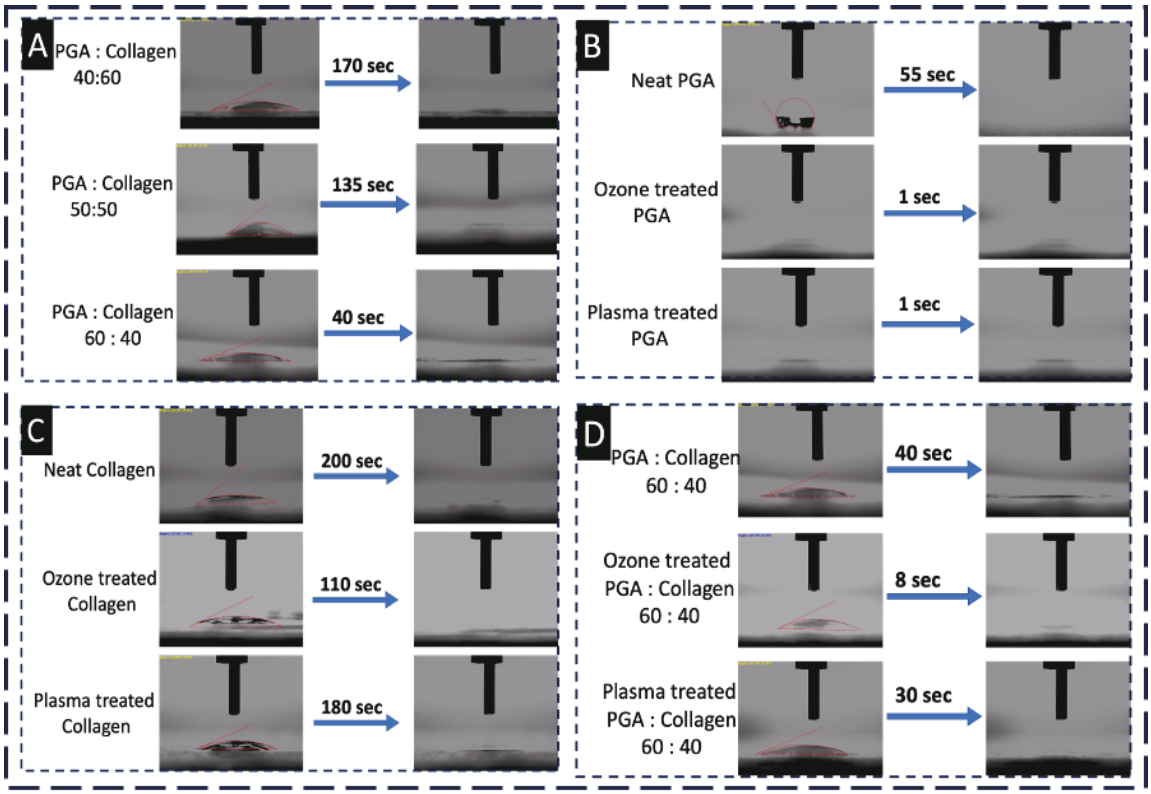

Fig.4.5. WCA test of (A) PGA/collagen nanofibers with blend ratios 40:60, 50:50 and 60:40, WCA of untreated, Ozone (O3) treated, and Plasma (N) treated (B) Neat PGA, (C) Neat collagen and (D) PGA/collagen 60:40.

4.4.4.2. Effect of SuPMA Incorporation and Cage-type Collector on Wettability of Blend Nanofibers

WCA of the cage-type PGA/collagen 60:40 blend is revealed in Fig.4.6A which interestingly showed more hydrophilicity compared to the smooth textured blend prepared on plain collector. Cage-type blend took only 35s to get the contact angle to reach 0° from 35.4°. Increased hydrophilicity is the target of preparing a cage-type blend, which may be ultimately advantageous to cell adhesion properties. Additionally, the wettability of neat cage-type blend and SuPMA incorporated blend is compared in Fig.4.6A, the incorporation of SuPMA 3% and SuPMA 5% showed super hydrophilic behavior on the surface of the blend which only took 2s and ≤1 s, respectively for the complete water droplet absorption on their surfaces while the contact angle was 10°. The reason behind the increased hydrophilicity is given in Fig.4.6 B and C showing FTIR and Raman spectroscopies, respectively to assess chemical groups available on the surface of the cage-type blend, and to confirm the extent of incorporation of SuPMA.

FTIR showed increasing peaks at 1400cm^{-1} on the incorporation of SuPMA, which reveals more OH groups on the surface of 3% SuPMA incorporated blend with increased hydrophilicity compared to neat cage-type blend and comparatively less hydrophilicity than the sample incorporated with 5% SuPMA. The reason of increased hydrophilicity and extent of incorporation of SuPMA was further confirmed by Raman spectroscopy, which reveals a continued increase in CH groups with stretching peaks at 2961cm^{-1} and 2967cm^{-1}. Raman spectrum also confirmed the presence of C=O, N–C=O and increased CH_2 at 1781cm^{-1}, 1659cm^{-1} and 1425cm^{-1} respectively. As per previous reports, increased number of CH_2 groups on polymeric fiber surfaces results in increased cell adhesion properties, which indicates the potential for cell culture applications of this optimized cage-type blend with 5% SuPMA content [59].

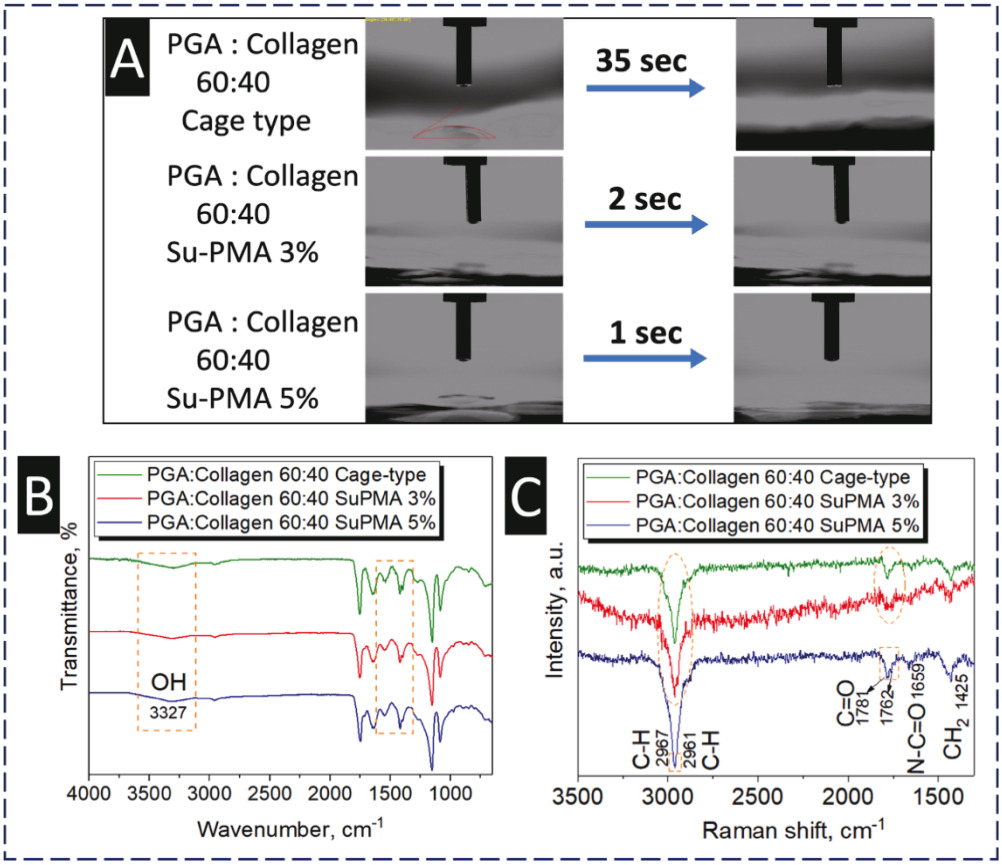

Fig.4.6. (A) WCA test of Cage-type PGA/collagen 40:60, (B) FTIR spectra of Cage-type PGA/collagen 40:60 with 3% SuPMA and cage-type PGA/collagen 40:60 with 5% SuPMA and (C) Raman spectra of Cage-type PGA/collagen 40:60 with 3% SuPMA and cage-type PGA/collagen 40:60 with 5% SuPMA.

4.5. Conclusion

The cage-type blended composition of PGA/collagen nanofibers with ratio 60:40 was optimized to achieve the maximum wettability with good handling properties. Optimized PGA/collagen with the ratio 60:40 showed a smooth morphology, whereas other blended PGA/collagen compositions did not resist the ozonation and plasma treatments pressure. FTIR and SEM-EDS revealed the presence of both PGA and collagen in the resultant blended composition, whereas the optimized blend with a ratio of 60:40 showed more NH and OH chemical groups on its surface, which was the reason behind its increased wettability. The optimized blend of PGA/collagen nanofibers was individually treated under plasma and ozonation, which potentially enhanced the wettability on the surface of pristine nanofibers and blends of PGA and collagen nanofibers. The ozone-treated optimized blend took 8s for droplet absorption to be complete, whereas the plasma-treated sample took 30s to reach the contact angle of 0°. A cage-type collector with pore size $2\times2mm^2$ for electrospinning was used as a collector to obtain robust nanofibers texture in order to impart handling flexibility, which interestingly increased the wettability of the optimized blend and took 5s for water droplet absorption to be complete on the surface, as per WCA results. SuPMA with 5% of incorporation in the optimized blend resulted in super hydrophilicity with a contact angle of 10°, and complete droplet absorption within 1s.

4.6. References

1. Lim, H.; Kim, H.S.; Qazi, R.; Kwon, Y.; Jeong, J.; Yeo, W. Advanced soft materials, sensor integrations, and applications of wearable flexible hybrid electronics in healthcare, energy, and environment. *Adv. Mater.* 2020, *32*, 1901924.
2. Sinha, R.; Cámara-Torres, M.; Scopece, P.; Falzacappa, E.V.; Patelli, A.; Moroni, L.; Mota, C. A hybrid additive manufacturing platform to create bulk and surface composition gradients on scaffolds for tissue regeneration. *Nat. Commun.* 2021, *12*, 500.
3. Pushp, P.; Gupta, M.K. Cardiac Tissue Engineering: A Role for Natural Biomaterials. In *Bioactive Natural Products for Pharmaceutical Applications*; Springer: Berlin/Heidelberg, Germany, 2021; pp. 617–641.
4. Ibrahim, H.M.; Klingner, A. A review on electrospun polymeric nanofibers: Production parameters and potential applications. *Polym. Test.* 2020, *90*, 106647.
5. Deng, X.; Qasim, M.; Ali, A. Engineering and polymeric composition of drug-eluting suture: A review. *J. Biomed. Mater. Res. Part A* 2021, *109*, 2065–2081.
6. Daniel, S. Biodegradable Polymeric Materials for Medicinal Applications. In *Green Composites*; Springer: Berlin/Heidelberg, Germany, 2021; pp. 351–372.
7. Baldwin, A.; Uy, L.; Booth, B.W. Characterization of collagen type I/tannic acid beads as a cell scaffold. *J. Bioact. Compat. Polym.* 2021, *36*, 124–138.

8. Tian, F.; Hosseinkhani, H.; Hosseinkhani, M.; Khademhosseini, A.; Yokoyama, Y.; Estrada, G.G.; Kobayashi, H. Quantitative analysis of cell adhesion on aligned micro- and nanofibers. *J. Biomed. Mater. Res. Part A* 2008, *84*, 291–299.
9. Sekiya, N.; Ichioka, S.; Terada, D.; Tsuchiya, S.; Kobayashi, H. Efficacy of a poly glycolic acid (PGA)/collagen composite nanofibre scaffold on cell migration and neovascularisation in vivo skin defect model. *J. Plast. Surg. Hand Surg.* 2013, *47*, 498–502.
10. Sayanagi, J.; Tanaka, H.; Ebara, M.; Okada, K.; Oka, K.; Murase, T.; Yoshikawa, H. Combination of electrospun nanofiber sheet incorporating methylcobalamin and PGA-collagen tube for treatment of a sciatic nerve defect in a rat model. *JBJS* 2020, *102*, 245–253.
11. Kobayashi, H.; Terada, D.; Yokoyama, Y.; Moon, D.W.; Yasuda, Y.; Koyama, H.; Takato, T. Vascular-inducing poly (glycolic acid)-collagen nanocomposite-fiber scaffold. *J. Biomed. Nanotechnol.* 2013, *9*, 1318–1326.
12. Shuai, C.; Yang, W.; Feng, P.; Peng, S.; Pan, H. Accelerated degradation of HAP/PLLA bone scaffold by PGA blending facilitates bioactivity and osteoconductivity. *Bioact. Mater.* 2021, *6*, 490–502.
13. Sharma, U.; Concagh, D.; Core, L.; Kuang, Y.; You, C.; Pham, Q.; Zugates, G.; Busold, R.; Webber, S.; Merlo, J. The development of bioresorbable composite polymeric implants with high mechanical strength. *Nat. Mater.* 2018, *17*, 96–103.
14. Park, K.I.; Teng, Y.D.; Snyder, E.Y. The injured brain interacts reciprocally with neural stem cells supported by scaffolds to reconstitute lost tissue. *Nat. Biotechnol.* 2002, *20*, 1111–1117.
15. Sun, A.; He, X.; Li, L.; Li, T.; Liu, Q.; Zhou, X.; Ji, X.; Li, W.; Qian, Z. An injectable photopolymerized hydrogel with antimicrobial and biocompatible properties for infected skin regeneration. *NPG Asia Mater.* 2020, *12*, 25.
16. Low, Y.J.; Andriyana, A.; Ang, B.C.; Zainal Abidin, N.I. Bioresorbable and degradable behaviors of PGA: Current state and future prospects. *Polym. Eng. Sci.* 2020, *60*, 2657–2675.
17. El-Ghazali, S.; Khatri, M.; Hussain, N.; Khatri, Z.; Yamamoto, T.; Kim, S.H.; Kobayashi, S.; Kim, I.S. Characterization and biocompatibility evaluation of artificial blood vessels prepared from pristine poly (Ethylene-glycol-co-1, 4-cyclohexane dimethylene-co-isosorbide terephthalate), poly (1, 4 cyclohexane di-methylene-co-isosorbide terephthalate) nanofi. *Mater. Today Commun.* 2021, *26*, 102113.
18. Langston, C.; Patterson, K.; Dishop, M.K.; Baker, P.; Chou, P.; Cool, C.; Coventry, S.; Cutz, E.; Davis, M.; Deutsch, G. A protocol for the handling of tissue obtained by operative lung biopsy: Recommendations of the child pathology co-operative group. *Pediatr. Dev. Pathol.* 2006, *9*, 173–180.
19. Coemert, S.; Roth, R.; Strauss, G.; Schmitz, P.M.; Lueth, T.C. A handheld flexible manipulator system for frontal sinus surgery. *Int. J. Comput. Assist. Radiol. Surg.* 2020, *15*, 1549–1559.
20. Wen, N.; Zhang, L.; Jiang, D.; Wu, Z.; Li, B.; Sun, C.; Guo, Z. Emerging flexible sensors based on nanomaterials: Recent status and applications. *J. Mater. Chem. A* 2020, *8*, 25499–25527.
21. Farmer, Z.-L.; Domínguez-Robles, J.; Mancinelli, C.; Larrañeta, E.; Lamprou, D.A. Urogynecological surgical mesh implants: New trends in materials, manufacturing and therapeutic approaches. *Int. J. Pharm.* 2020, *585*, 119512.
22. Samantaray, P.K.; Little, A.; Haddleton, D.M.; McNally, T.; Tan, B.; Sun, Z.; Huang, W.; Ji, Y.; Wan, C. Poly (glycolic acid)(PGA): A versatile building block expanding high performance and sustainable bioplastic applications. *Green Chem.* 2020, *22*, 4055–4081.

23. Liu, L.; Stephens, B.; Bergman, M.; May, A.; Chiang, T. Role of collagen in airway mechanics. *Bioengineering* 2021, *8*, 13.
24. Kanzaki, M.; Takagi, R.; Washio, K.; Kokubo, M.; Mitsuboshi, S.; Isaka, T.; Yamato, M. Bio-artificial pleura using autologous dermal fibroblast sheets to mitigate air leaks during thoracoscopic lung resection. *Regen. Med.* 2021, *6*, 2.
25. Charlton, N.P.; Swain, J.M.; Brozek, J.L.; Ludwikowska, M.; Singletary, E.; Zideman, D.; Epstein, J.; Darzi, A.; Bak, A.; Karam, S. Control of severe life-threatening external bleeding in the out-of-hospital setting: A systematic review. *Prehosp. Emerg. Care* 2021, *25*, 235–267.
26. Madhumanchi, S.; Srichana, T.; Domb, A.J. Polymeric Biomaterials. In *Biomedical Materials*; Springer: Berlin/Heidelberg, Germany, 2021; pp. 49–100.
27. Christoff-Tempesta, T.; Cho, Y.; Kim, D.-Y.; Geri, M.; Lamour, G.; Lew, A.J.; Zuo, X.; Lindemann, W.R.; Ortony, J.H. Self-assembly of aramid amphiphiles into ultra-stable nanoribbons aligned nanoribbon threads. *Nat. Nanotechnol.* 2021, *16*, 447–454.
28. Akoumeh, R.; Elzein, T.; Martínez-Campos, E.; Reviriego, F.; Rodríguez-Hernández, J. Fabrication of porous films from immiscible polymer blends: Role of the surface structure on the cell adhesion. *Polym. Test.* 2020, *91*, 106797.
29. Bilginer, R.; Ozkendir-Inanc, D.; Yildiz, U.H.; Arslan-Yildiz, A. Biocomposite scaffolds for 3D cell culture: Propolis enriched polyvinyl alcohol nanofibers favoring cell adhesion. *J. Appl. Polym. Sci.* 2021, *138*, 50287.
30. Balu, R.; Dutta, N.K.; Dutta, A.K.; Choudhury, N.R. Resilin-mimetics as a smart biomaterial platform for biomedical applications. *Nat. Commun.* 2021, *12*, 149.
31. Daum, R.; Mrsic, I.; Hutterer, J.; Junginger, A.; Hinderer, S.; Meixner, A.J.; Gauglitz, G.; Chassé, T.; Schenke-Layland, K. Fibronectin adsorption on oxygen plasma-treated polyurethane surfaces modulates endothelial cell response. *J. Mater. Chem. B* 2021, *9*, 1647–1660.
32. Alves, C.M.; Yang, Y.; Carnes, D.L.; Ong, J.L.; Sylvia, V.L.; Dean, D.D.; Agrawal, C.M.; Reis, R.L. Modulating bone cells response onto starch-based biomaterials by surface plasma treatment and protein adsorption. *Biomaterials* 2007, *28*, 307–315.
33. Khorasani, M.T.; Mirzadeh, H.; Irani, S. Plasma surface modification of poly (l-lactic acid) and poly (lactic-co-glycolic acid) films for improvement of nerve cells adhesion. *Radiat. Phys. Chem.* 2008, *77*, 280–287.
34. Poncin-Epaillard, F.; Legeay, G. Surface engineering of biomaterials with plasma techniques. *J. Biomater. Sci. Polym. Ed.* 2003, *14*, 1005–1028.
35. Kasai, K.; Kimura, Y.; Miyata, S. Improvement of adhesion and proliferation of mouse embryonic stem cells cultured on ozone/UV surface-modified substrates. *Mater. Sci. Eng. C* 2017, *78*, 354–361.
36. Mao, C.; Qiu, Y.; Sang, H.; Mei, H.; Zhu, A.; Shen, J.; Lin, S. Various approaches to modify biomaterial surfaces for improving hemocompatibility. *Adv. Colloid Interface Sci.* 2004, *110*, 5–17.
37. Khan, M.Q.; Lee, H.; Khatri, Z.; Kharaghani, D.; Khatri, M.; Ishikawa, T.; Im, S.-S.; Kim, I.S. Fabrication and characterization of nanofibers of honey/poly (1, 4-cyclohexane dimethylene isosorbide trephthalate) by electrospinning. *Mater. Sci. Eng. C* 2017, *81*, 247–251.
38. Phan, D.-N.; Rebia, R.A.; Saito, Y.; Kharaghani, D.; Khatri, M.; Tanaka, T.; Lee, H.; Kim, I.-S. Zinc oxide nanoparticles attached to polyacrylonitrile nanofibers with hinokitiol as gluing agent for synergistic antibacterial activities and effective dye removal. *J. Ind. Eng. Chem.* 2020, *85*, 258–268.

39. Hussain, N.; Ullah, S.; Sarwar, M.N.; Hashmi, M.; Khatri, M.; Yamaguchi, T.; Khatri, Z.; Kim, I.S. Fabrication and Characterization of Novel Antibacterial Ultrafine Nylon-6 Nanofibers Impregnated by Garlic Sour. *Fibers Polym.* 2020, *21*, 2780–2787.
40. Sabra, S.; Ragab, D.M.; Agwa, M.M.; Rohani, S. Recent advances in electrospun nanofibers for some biomedical applications. *Eur. J. Pharm. Sci.* 2020, *144*, 105224.
41. Leung, V.; Ko, F. Biomedical applications of nanofibers. *Polym. Adv. Technol.* 2011, *22*, 350–365.
42. Khatri, M.; Ahmed, F.; Jatoi, A.W.; Mahar, R.B.; Khatri, Z.; Kim, I.S. Ultrasonic dyeing of cellulose nanofibers. *Ultrason. Sonochem.* 2016, *31*, 350–354.
43. Qureshi, U.A.; Khatri, Z.; Ahmed, F.; Khatri, M.; Kim, I.-S. Electrospun zein nanofiber as a green and recyclable adsorbent for the removal of reactive black 5 from the aqueous phase. *ACS Sustain. Chem. Eng.* 2017, *5*, 4340–4351.
44. Khatri, M.; Khatri, Z.; El-Ghazali, S.; Hussain, N.; Qureshi, U.A.; Kobayashi, S.; Ahmed, F.; Kim, I.S. Zein nanofibers via deep eutectic solvent electrospinning: Tunable morphology with super hydrophilic properties. *Sci. Rep.* 2020, *10*, 15307.
45. Ibupoto, A.S.; Qureshi, U.A.; Ahmed, F.; Khatri, Z.; Khatri, M.; Maqsood, M.; Brohi, R.Z.; Kim, I.S. Reusable carbon nanofibers for efficient removal of methylene blue from aqueous solution. *Chem. Eng. Res. Des.* 2018, *136*, 744–752.
46. Khatri, M.; Hussain, N.; El-Ghazali, S.; Yamamoto, T.; Kobayashi, S.; Khatri, Z.; Ahmed, F.; Kim, I.S. Ultrasonic-assisted dyeing of silk fibroin nanofibers: An energy-efficient coloration at room temperature. *Appl. Nanosci.* 2020, *10*, 917–930.
47. Qureshi, U.A.; Khatri, Z.; Ahmed, F.; Ibupoto, A.S.; Khatri, M.; Mahar, F.K.; Brohi, R.Z.; Kim, I.S. Highly efficient and robust electrospun nanofibers for selective removal of acid dye. *J. Mol. Liq.* 2017, *244*, 478–488.
48. Khatri, M.; Ahmed, F.; Shaikh, I.; Phan, D.-N.; Khan, Q.; Khatri, Z.; Lee, H.; Kim, I.S. Dyeing and characterization of regenerated cellulose nanofibers with vat dyes. *Carbohydr. Polym.* 2017, *174*, 443–449.
49. Xia, H.; Li, X.; Gao, W.; Fu, X.; Fang, R.H.; Zhang, L.; Zhang, K. Tissue repair and regeneration with endogenous stem cells. *Nat. Rev. Mater.* 2018, *3*, 174–193.
50. Mohammadinejad, R.; Kumar, A.; Ranjbar-Mohammadi, M.; Ashrafizadeh, M.; Han, S.S.; Khang, G.; Roveimiab, Z. Recent advances in natural gum-based biomaterials for tissue engineering and regenerative medicine: A review. *Polymers* 2020, *12*, 176.
51. Khajavi, R.; Abbasipour, M.; Bahador, A. Electrospun biodegradable nanofibers scaffolds for bone tissue engineering. *J. Appl. Polym. Sci.* 2016, *133*, 42883.
52. Arima, Y.; Iwata, H. Effect of wettability and surface functional groups on protein adsorption and cell adhesion using well-defined mixed self-assembled monolayers. *Biomaterials* 2007, *28*, 3074–3082.
53. Xun, X.; Wan, Y.; Zhang, Q.; Gan, D.; Hu, J.; Luo, H. Low adhesion superhydrophobic AZ31B magnesium alloy surface with corrosion resistant and anti-bioadhesion properties. *Appl. Surf. Sci.* 2020, *505*, 144566.
54. Dou, X.-Q.; Zhang, D.; Feng, C.-L. Wettability of supramolecular nanofibers for controlled cell adhesion and proliferation. *Langmuir* 2013, *29*, 15359–15366.
55. Yang, X.; Tu, Q.; Shen, X.; Pan, M.; Jiang, C.; Zhu, P.; Li, Y.; Li, P.; Hu, C. Surface modification of Poly (p-phenylene terephthalamide) fibers by polydopamine-polyethyleneimine/graphene oxide multilayer films to enhance interfacial adhesion with rubber matrix. *Polym. Test.* 2019, *78*, 105985.
56. Rezaei, S.M.; Ishak, Z.A.M. The biocompatibility and hydrophilicity evaluation of collagen grafted poly (dimethylsiloxane) and poly (2-hydroxyethylmethacrylate) blends. *Polym. Test.* 2011, *30*, 69–75.

57. Ngiam, M.; Liao, S.; Patil, A.J.; Cheng, Z.; Chan, C.K.; Ramakrishna, S. The fabrication of nano-hydroxyapatite on PLGA and PLGA/collagen nanofibrous composite scaffolds and their effects in osteoblastic behavior for bone tissue engineering. *Bone* 2009, *45*, 4–16.
58. Kajiyama, T.; Kobayashi, H.; Taguchi, T.; Saito, H.; Kamatsu, Y.; Kataoka, K.; Tanaka, J. Synthesis of activated poly (α, β-malic acid) using N-hydroxysuccinimide and its gelation with collagen as biomaterials. *Mater. Sci. Eng. C* 2004, *24*, 815–819.
59. El-Ghazali, S.; Khatri, M.; Mehdi, M.; Kharaghani, D.; Tamada, Y.; Katagiri, A.; Kobayashi, S.; Kim, I.S. Fabrication of Poly (Ethylene-glycol 1, 4-Cyclohexane Dimethylene-Isosorbide-Terephthalate) Electrospun Nanofiber Mats for Potential Infiltration of Fibroblast Cells. *Polymers* 2021, *13*, 1245.

CHAPTER 5 Conclusion

5.1. Conclusion

In this dissertation, a variety of polymeric nanofibers were successfully prepared using the blend electrospinning method. In the first chapter, a blend of PICT and PEICT nanofibers with 50:50 ratio was prepared for human breast cell culture and showed potential infiltration of about 87%. Based on AFM images showing the nanofibers surface topography, blended composition was comparatively better than pristine PICT and PEICT for the infiltration of human breast cells. The optimized blended nanofiber composite was used in tubular form with a cross-sectional diameter less than 2mm as three-dimensional scaffold with tunable tensile strength.

In this research PEICT nanofiber mat did not show good infiltration of human breast cells on its surface, therefore in the second chapter PEICT was explored for fibroblast cell adhesion and cell viability. Because of the bigger size of fibroblast, the polymer concentration of PEICT for electrospinning was increased to 11% from 10% to get a slightly bigger average diameter size, which showed 90% adhesion of fibroblast cells revealing its biomedical potential. On the other hand, nanofibers at 11% polymer concentration did not show any negative influence on the morphology of PEICT nanofibers. Additionally, XPS spectroscopy was performed for PEICT ENM to support FTIR data. Cell adhesion was revealed with respect to surface characteristics of PEICT ENM.

In both second and third chapters, cell infiltration of two different cell types on different bio-based polymers has been reported with respect to surface properties. Thus, in the fourth chapter we chose to investigate the surface characteristics of biocompatible polymers already explored for cell culture without revising cell culture experiments.

PGA and Collagen polymers were selected for this research because they are being widely explored for their biocompatibility and cell culture applications.

The fourth chapter is a detailed investigation of surface modification using two different methods and blend electrospinning technique. PGA/Collagen blended composition with ratio 60:40 was observed as optimized with respect to handling properties; the samples were ozonated, plasma treated and incorporated with SuPMA to improve their surface wettability assessed under WCA. Additionally, the surface texture of PGA/Collagen 60:40 was improved by using a cage-type collector for electrospinning.

Conclusively, surface damaging caused by expensive surface treatments can be avoided by using a simple blend electrospinning technique which can effectively alter the surface wettability and texture (smoothness/compactness) by blend ratio optimization.
Conclusively, PICT/PEICT (50:50), PEICT (11%), and PGA/Collagen (60:40) nanofibers have showed the potential to be used as biomaterials for cell culture applications.

5.2. Future Suggestion

The optimized blended compositions based on PGA, Collagen, PICT and PEICT from the current research can be used to explore cell viability and adhesion of other types of cells including smooth muscle, osteoblasts or endothelial cells. These compositions can further be improved by incorporation of different natural medicinal ingredients such as turmeric, ginger, artemisia, aloe-vera, argan oil or synthetic drugs for wound dressing such as antioxidants, antibacterial drugs or antiviral drugs.
These composites can be explored for advanced biomedical smart apparel applications. In addition, because of the considerable properties of these composites, they can be further explored for other research fields where these surface properties are required.

Accomplishments

Publications

1- **El-Ghazali, S.**, Khatri, M., Hussain, N., Khatri, Z., Yamamoto, T., Kim, S. H., Kobayashi, S. Kim, I. S. (2021). Characterization and biocompatibility evaluation of artificial blood vessels prepared from pristine poly (Ethylene-glycol-co-1, 4-cyclohexane dimethylene-co-isosorbide terephthalate), poly (1, 4 cyclohexane di-methylene-co-isosorbide terephthalate) nanofibers and their blended composition. *Materials Today Communications*, *26*, 102113.

2- **El-Ghazali, S.**, Khatri, M., Mehdi, M., Kharaghani, D., Tamada, Y., Katagiri, A., Kobayashi, S. Kim, I. S. (2021). Fabrication of Poly (Ethylene-glycol 1, 4-Cyclohexane Dimethylene-Isosorbide-Terephthalate) Electrospun Nanofiber Mats for Potential Infiltration of Fibroblast Cells. *Polymers*, *13*(8), 1245.

3- **El-Ghazali, S.**, Kobayashi, H., Khatri, M., Phan, D. N., Khatri, Z., Mahar, S. K., Kobayashi, S. Kim, I. S. (2021). Preparation of a Cage-Type Polyglycolic Acid/Collagen Nanofiber Blend with Improved Surface Wettability and Handling Properties for Potential Biomedical Applications. *Polymers*, *13*(20), 3458.

4- Khatri, M., Hussain, N., **El-Ghazali, S.**, Yamamoto, T., Kobayashi, S., Khatri, Z., Ahmed, F. Kim, I. S. (2020). Ultrasonic-assisted dyeing of silk fibroin nanofibers: An energy-efficient coloration at room temperature. *Applied Nanoscience*, *10*(3), 917-930.

5- Khatri, M., Khatri, Z., **El-Ghazali, S.**, Hussain, N., Qureshi, U. A., Kobayashi, S., Ahmed, F. Kim, I. S. (2020). Zein nanofibers via deep eutectic solvent electrospinning: tunable morphology with super hydrophilic properties. *Scientific reports*, *10*(1), 1-11.

6- Book chapter accepted for publication:
El-Ghazali, S., Khatri, M., Kobayashi, S., Kim, I.S. (2021). An overview of medical textile materials. Elsevier. (3).

Prize/Award

International Conferences (Best Poster presentation Award)

1- El-Ghazali Sofia, Shunichi Kobayashi, Ick Soo Kim. Tubular scaffolds for biomedical application. “Chemical Engineering and Catalysists”. London, UK (2019/12/12)

2- El-Ghazali Sofia, Shunichi Kobayashi, Ick Soo Kim. Three-dimensional artificial scaffold for biomedical applications using nanfibers. “Nano engineering and Pharma” Dubai, UAE (2018/09/24).

Acknowledgements

All praises to Allah almighty, the most merciful and the most gracious. I would like to thank, at first place, my advisor, Prof. Shunichi Kobayashi for his consistent support during 5 years, his technical guidance and precious advices to accomplish my goal. I would also like to thank Prof. Kim Ick Soo for the effective collaboration for the development of my research.

I cannot forget to praise my parents, who gave me the vision to always target bigger opportunities and provided a ground to succeed in my life. The completion of my dissertation would not have been possible without the support and nurturing of my husband Muzamil Khatri and the smile of my daughter Samiya.

My profound gratitude would be to Prof. Makoto Shimosaka - Program Director and previous Dean of the Faculty of Textile Science and Technology for his contributions to the Leading Program and also to Prof. Hideaki Morikawa, the current Dean of the Faculty.
I am deeply thankful to Prof. Mikihiko Miura and Prof. Tsutomu Ishiwatari, Prof. Hiroaki Ishizawa, Prof. Masayuki Takatera and Prof. Shigeru Inui for their guidance, counselling and help. I would like to express my deepest appreciation to Ms. Akiko Kubota, Ms. Tomoko Ikeda and Ms. Naoko Suguta, Leading Program staff, who supported me in all the difficult conditions and helped me during my studies at Shinshu University.

My sincere thanks to Prof. Kim Seung Hun for guiding me during the academic internship at Hanyang University. I am deeply indebted to Prof. Michael James Andrew Honywood for counseling and help at difficult parts of my 5 years in Japan. I would also like to extend my sincere thanks to all my lab colleagues for their technical assistance and for allowing me to work in a very friendly environment. I am also grateful to all Leading Program students, my friends and cousins.

Last but not least, I would like to thank Shinshu University Advanced Leading Graduate Program as well as the Ministry of Education, Culture, Sports, Science and Technology (MEXT) and Rotary Yoneyama for the financial support.